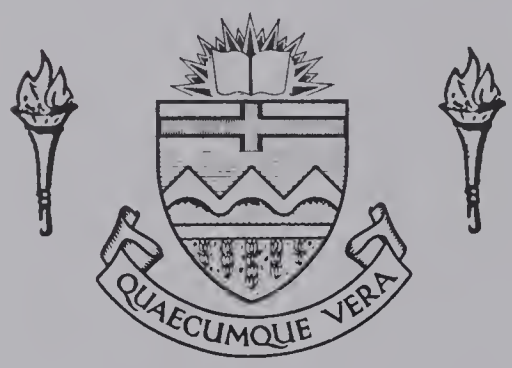


*The University of Alberta*
*Printing Department*
*Edmonton, Alberta*

THE UNIVERSITY OF ALBERTA

# SURGES IN ICE COVERED CHANNELS

by

© DONALD MARLIN LILAND

A THESIS

SUBMITTED TO THE FACULTY OF GRADUATE STUDIES

IN PARTIAL FULFILMENT OF THE REQUIREMENTS FOR THE DEGREE OF

MASTER OF SCIENCE

DEPARTMENT OF CIVIL ENGINEERING

EDMONTON, ALBERTA

Spring 1971

UNIVERSITY OF ALBERTA

FACULTY OF GRADUATE STUDIES

The undersigned certify that they have read, and recommend to the Faculty of Graduate Studies for acceptance, a thesis entitled,

SURGES IN ICE COVERED CHANNELS

submitted by Donald Marlin Liland in partial fulfilment of the requirements for the degree of Master of Science.

## ABSTRACT

This thesis summarizes an investigation on the effect of an ice cover on open channel surges. The effect of ice on total channel friction is analyzed first and this is then applied to open channel surges.

The propagation of surges is calculated by means of the method of characteristics. With the use of numerical techniques, the computer is employed to solve the characteristic equations. The behavior of surges is tested under various channel conditions.

A radical change in the profile and propagation velocity of a surge is observed with the addition of an ice cover to a channel.

ACKNOWLEDGEMENTS

The author wishes to extend his appreciation to Professor J. B. Nuttall for his guidance and constructive criticism rendered throughout the project.

Water Survey of Canada and Calgary Power gave valuable assistance in supplying flow data and channel geometry for the tests.

# TABLE OF CONTENTS

PAGE

PAGE

# LIST OF TABLES

# LIST OF FIGURES

FIGURE PAGE

# GLOSSARY OF SYMBOLS

A - cross-sectional area of flow.

B - top width of flow.

Co - wave propagation velocity.

$Co^+$ - positive characteristic curve.

$Co^-$ - negative characteristic curve.

d - depth of flow under open water conditions.

$d_1$ - depth of flow under ice covered conditions.

f - friction factor.

F - water surface fall.

g - acceleration due to gravity.

H - stage.

k - sliding coefficient - ratio of the discharge under ice to open water discharge at the same stage.

$k_s$ - relative roughness height.

L,M - points of known conditions.

n - Manning's roughness factor for the total cross-section.

$n_1$ - Manning's roughness factor for ice boundary.

$n_2$ - Manning's roughness factor for bed boundary.

N - point of unknown conditions.

P - wetted perimeter.

Q - discharge

R - hydraulic radius.

S - water surface slope.

$S_f$ - slope of energy grade line.

So - bed slope.

$t, T$ - time.

$t_i$ - bouyant thickness of ice.

$U$ - velocity at a point.

$U_*$ - shear velocity.

$V$ - average cross-sectional velocity.

$x, X$ - distance along channel.

$y, Y$ - measurement of depth at point velocities.

$y_1$ - distance from ice boundary to point of maximum velocity.

$y_2$ - distance from bed boundary to point of maximum velocity.

$z$ - channel bottom elevation.

$\alpha, \beta, \lambda$ - constants.

$\gamma$ - unit weight of water.

$\tau$ - bed shear stress.

# CHAPTER I

## INTRODUCTION

### 1.1 The Problem

On northern rivers, dams are required for the regulation of flow and the generation of hydro-electric power. To meet these demands, which are greatest during the winter, the release of large quantities of water is required. The hydro-electric power is used for the peak daily electrical loads thus, resulting in the periodic release of water. This rapid change in the flow rate causes a surge to form and propagate through the channel downstream from the dam. Since the advent of the high-speed digital computer, there has been considerable use of numerical techniques for the solution of engineering problems. Recently these methods have been used in the simulation of open channel wave problems. However, they have only been applied to short channels having a free water surface condition. In areas of cold winters the rivers and streams are covered with ice having appreciable thickness and structural strength. These numerical techniques have not as yet been applied to surges under an ice cover.

The present investigation was carried out in an attempt to develop a means of predicting the behaviour of surges under these conditions. Presently, in Alberta, the releases from the Brazeau Dam propagating down the Brazeau and North Saskatchewan Rivers are of particular interest. More dams are planned for these areas resulting in a greater need for a knowledge of the behavior of surges under ice cover.

## 1.2 Purpose and Scope

The purpose herein was to simulate, on the digital computer, surges propagating down an ice covered prismatic channel. From this simulation the effect of a surface ice cover, having structural strength, on the behavior of open channel surges could be studied. The main objectives of the study were:

1. To determine the effect of channel roughness on open channel surges.
2. To determine the physical behavior of open channel surges under surface ice cover conditions.

In order to simulate an ice covered channel it was necessary to determine the effect of the ice on the roughness of the channel. Therefore, the investigation initially dealt with ice roughness and later surges were considered. The scope of the investigation was limited by the lack of time and equipment for obtaining roughness measurements as well as the limit on computer time in order that the simulation be economically feasible for future use.

Data on the channel roughness was the first to be obtained. Continuous stage readings were recorded throughout the ice cover period. These were related to discharge readings taken at a section of the river which was ice free. During mid-winter velocity profiles were taken to obtain additional data on the effects of ice cover on the total roughness of the channel.

Using numerical techniques and the digital computer, a simulation of surges propagating down a channel was made. Runs were carried out under different flow rates and different channel roughnesses. As many as

possible of these runs were compared to actual data available on surges on the North Saskatchewan River.

# CHAPTER II

# FRICTION FACTOR FOR STEADY FLOW UNDER ICE COVER

## 2.1 General

For a given discharge, an ice-covered river maintains a higher stage than an uncovered river. Part of this increase in stage is due to the bouyant thickness "$t_i$" of the ice cover. The free surface of the water is raised approximately $0.9t_i$; the numerical coefficient depends on the ice density. An additional stage increase is caused by the increase in frictional resistance due to the roughness of the underside of the ice. The effect of the increase in friction is to reduce the velocity from that of the uncovered channel with an equivalent stage. To compensate for the decrease in velocity, the cross-sectional area must increase, thus increasing the stage. The total increase in stage due to the ice cover, from the stage for the same open water discharge, is usually referred to as backwater. This backwater changes during the ice cover period since the ice is a variable feature in the channel. During freeze-up, there is a large but undefined increase in friction. This friction decreases and is rather stable during midwinter. Preceeding break-up there is again a poorly defined rise in frictional effects. Some methods of relating the stage to discharge have been proposed but all give limited success.

## 2.2 Literature Review

A review of the literature indicates that very little work has been done in this field due to the many variables involved and the difficulty

in obtaining data during ice cover. The majority of the work only considers a general increase in stage due to the ice cover, with little consideration given to the causes of this increase.

Tillinghast (1905) did a study on six rivers which had varying discharges from 100 to 6000 cfs. From his studies, he found that it was more reliable to use gauge to the water surface rather than to the under surface of the ice. The sliding coefficient "k", which is the ratio of measured discharge to open water discharge at the same stage, was found to vary between 0.30 and 0.75 throughout the season.

In studying the complex manner in which ice forms, Hoyt (1913) found that each stream presented different conditions, therefore making it difficult to formulate one method for calculating discharge. He proposed three methods:

(i) Water surface gauge readings may be applied directly to the open water rating curve provided the stream is open at the control section and no backwater exists at the gauge.

(ii) Water surface gauge readings may be applied directly to a special rating curve based on winter discharge measurements.

(iii) Discharge measurements may be used in connection with gauge heights and data showing climatic conditions and the occurrence of ice.

In using a backwater correction, Kolupaila (1938) saw a correlation between the correction and air temperature. He concluded that "the relation between winter and summer discharges depends on three factors: (i) the pecularities of the roughness of the ice and bed (ii) the different slopes of the water level and (iii) the thickness of the ice in relation

to the depth." He found that k drops from 1.0 to 0.2 or 0.3 during freeze-up, then increases slowly all winter and rapidly rises to 1.0 as break-up occurs. He proposed that three measurements of discharge be made, the first right after freeze-up and two subsequent ones during the winter, thus enabling the value of the k to be determined.

Anchor ice is ice which forms on underwater rocks. This formation is a result of cooling the underwater surfaces below the freezing point by a slight supercooling of the water. The coating of anchor ice may be several inches thick thus causing the stage to rise. An increase in stage due to anchor ice will not occur in ice covered channels since the ice cover effectively cuts down the supercooling of the water (Chow 1964).

Carey (1967) observed ripplelike and dunelike features on the underside of the ice cover. From his observations he developed two methods of calculating discharge: the stage-fall-relation method and the pipe-flow method. The first method basically involves two graphical relationships: (1) a relation between stage and discharge for some fixed condition of fall of the water surface and (2) a relation between discharge ratios and corresponding fall ratios. If the fall is not constant with stage an additional graphical relationship is required between stage and fall. The method depends on the principle that:

$$\frac{Q_1}{Q_2} = \text{function}\left(\frac{F_1}{F_2}\right) \quad \text{- - - - - - - - - - - - - - - - - - - - -(2.1)}$$

where $Q_1$ and $Q_2$ are different discharges and $F_1$ and $F_2$ are the corresponding falls of the water surface. The pipe-flow method makes use of a modified Darcy-Weisbach equation:

$$Q = \sqrt{\frac{8g}{f \text{ mod}}}\ AR^{\frac{1}{2}}\ S^{\frac{1}{2}} \quad \text{- - - - - - - - - - - - - - - - - - (2.2)}$$

where f mod is a modified friction factor, S is the water surface slope and $AR^{\frac{1}{2}}$ is the section factor. A modified friction factor is used to compensate for the fact that the water surface slope was used rather than the energy gradient. From the graphical relationships of modified friction factor versus water surface slope and section factor versus gauge height, the discharge is obtained. The stage-fall method is the more attractive of the two because it is more accurate and it requires less field and office work.

Some studies have been done on the calculation of a composite roughness for an ice covered channel, as part of the increase in the stage is due to the increase in roughness. In 1964, Nezkikhovskiy recommended three formulae for calculating a composite roughness factor for natural channels:

$$\text{Weighted average} \quad n = \frac{n_1 + n_2}{2} \qquad \text{- - - - - - - - - - - (2.3)}$$

$$\text{Pavolovskiy's} \quad n = 0.71\sqrt{n_1^2 + n_2^2} \qquad \text{- - - - - - - - - (2.4)}$$

$$\text{Belokon's - Sabaneer's} \quad n = 0.63 n_1 \left[1 + \left(\frac{n_2}{n_1}\right)^{1.5}\right]^{2/3} \qquad \text{- - (2.5)}$$

The weighted average method is correct only in form as it does not relate the roughness to the hydraulic radius. Pavlovskiy assumed that the total hydraulic radius was equal to the mean depth and also the hydraulic radii of the two different parts of roughness. He recognized his shortcomings and wrote that his formula is "useful only as a first approximation". The Belokon - Sabaneer method is the most accurate. It is, however, defective when the ice cover is ideally smooth and therefore it must only

be applied to closed channels with some roughness. With the above formulae, the discrepancy in the results of the computation of n with observed values of $n_1$ and $n_2$ was less than 9%.

In his studies of two power channels in Sweden, Larsen (1969) developed a composite roughness formula:

$$\frac{1}{n} = \frac{(y_1/y_2)^{5/3} \left(\frac{1}{n_1} + \frac{1}{n_2}\right)}{(1/2)^{2/3} (y_1/y_2 + 1)^{5/3}} \qquad \text{- - - - - - - - - - - - - - - - (2.6)}$$

where $y_1$ and $y_2$ are the distances from the bottom of the ice to the point of maximum velocity and from the bed to the point of maximum velocity, respectively. Assuming a logarithmic velocity distribution, he determined a roughness coefficient "$k_s$" for each part of the boundary. The roughness coefficient was then related to Manning's n by: $n = ck_s^{1/6}$. He also observed bed forms on the underside of the ice cover.

Recent studies have been carried out on the Peace River and Slave River in northern Alberta by the Arctic River Work Group of the Federal Department of Energy, Mines and Resources in Calgary. In 1966, Campbell realized that a single rating curve could not be used for the full duration of a winter. A two part rating curve (named the $W_A$ and $W_B$ method) was developed, with the periods chosen being, "freeze-up to the lowest winter gauge height" and "lowest winter gauge height to break-up". In comparing six methods, Morton (1967) found that the "Normal Backwater" method, which uses a backwater correction to the open channel rating curve, gave the best accuracy for winter streamflow. Bennett (1968) modified the $W_A$ and $W_B$ method to give the discharge equation:

$$Q = A_0 + A_1(\text{stage}) + A_2(\text{stage})^2 + A_3(\text{coded date}) + A_4(\text{cumulative degree - days since freeze-up}) \text{ - - - - - - - - - - - - -(2.7)}$$

He suggested that three discharge measurements be made during the winter to determine the values of A: (i) immediately after freeze-up (ii) approximately the time of minimum gauge height (iii) close to spring break-up.

Thus far, the major portion of the ice studies have been done during the middle portion of the winter. There has been some consideration of the break-up period but the freeze-up period has been omitted since the backwater is generally very erratic during this time. Climatic conditions, large increases in friction and ice jamming are all causes of the erratic backwater. It is unfortunate that this period has been omitted since its effects contribute to the condition of flow during the remainder of the ice cover period.

## 2.3 Theoretical Aspects of Determining Roughness from Measured Velocity Distribution.

The forming of an ice cover on a wide open channel causes a radical change in its hydraulic conditions. As a result of the ice cover, the open channel becomes a closed conduit. Its cross-sectional area adjusts to the need since the ice is a floating mass. This surface cover produces a large increase in the wetted perimeter. Generally the roughnesses of the two boundaries are not the same. Therefore, it becomes necessary to compute a composite roughness to determine the head losses.

Assuming the Prandtl-Karman equation for fully developed turbulent flow to be valid, the roughness of the boundary can be determined from the velocity distribution. The velocity distribution near the boundary is governed by the roughness and distance from the boundary according to:

$$\frac{U}{U*} = \alpha \log y/k_s + \beta \quad \text{- - - - - - - - - - - - - - - - - - - - - (2.8)}$$

From the experimental work of Nikuradse the values of $\alpha$ and $\beta$ are 5.75 and 8.5 respectively. Plotting the measured velocities on semi-logarithmic paper should produce a straight line. The slope of the line is equal to $5.75 \cdot U*$. Choosing U and a corresponding y, the equivalent roughness, $k_s$, can be determined by substitution into equation (2.8).

For rough turbulent flow in a wide channel, Keulegan (1938) showed that:

$$\frac{\overline{U}}{U*} = 6.0 + 5.75 \log \frac{y}{k_s} \quad \text{- - - - - - - - - - - - - - - - - - - - (2.9)}$$

Manning's formula for a wide channel can be written as:

$$\overline{U} = \frac{1.486}{n} y^{2/3} So^{1/2} \quad \text{- - - - - - - - - - - - - - - - - - - - (2.10)}$$

with $U*$ equal to $\sqrt{gySo}$ equation (2.10) can be rewritten as:

$$\frac{\overline{U}}{U*} = \frac{1.486}{n} \frac{1}{\sqrt{g}} y^{1/6} \quad \text{- - - - - - - - - - - - - - - - - - - - (2.11)}$$

Equating equations (2.9) and (2.11) results in:

$$n = \frac{1.486\, y^{1/6}}{\sqrt{g}\,(6.0 + 5.75 \log y/k_s)} \quad \text{- - - - - - - - - - - - - - - - - - - - (2.12)}$$

From the calculated values of y and $k_s$, a value for Manning's n can be calculated.

# CHAPTER III

# ANALYSIS OF ROUGHNESS UNDER ICE COVER

## 3.1 General

A preliminary study of the ice roughness on the North Saskatchewan River through Edmonton was carried out during the winter of 1969 - 70. The data collected consisted of continuous stage recordings taken throughout the ice cover period and velocity profiles taken during mid-winter. From this information the variation in roughness during the winter can be readily detected. A roughness coefficient was calculated for the mid-winter period. The data collected was not sufficient to give a complete analysis of the additional roughness due to the ice cover, but it gives a fair estimate of the roughness coefficient.

## 3.2 Collection of Data

At three sections in the ice covered portion of the river, stage readings were taken by continuous stage recorders. Two of the recorders were located in the wells of pumping stations while the other was located in a bridge pier. Figure 3-1 gives a plan of the North Saskatchewan River through Edmonton with the locations of the recorders labelled. The gauge located in the pier of the Quesnel Bridge operated only a short time after freeze-up and then it became frozen. Continuous pumping at varying rates existed at the California Standard Pumphouse. The unsteady pumping caused the well to have a varying amount of drawdown; therefore, inducing error into the stage recordings. The gauge located at Mayfair Park gave the most accurate readings of the three gauges. The occasional pumping which occurred at this gauge could be detected, thus the stage readings with

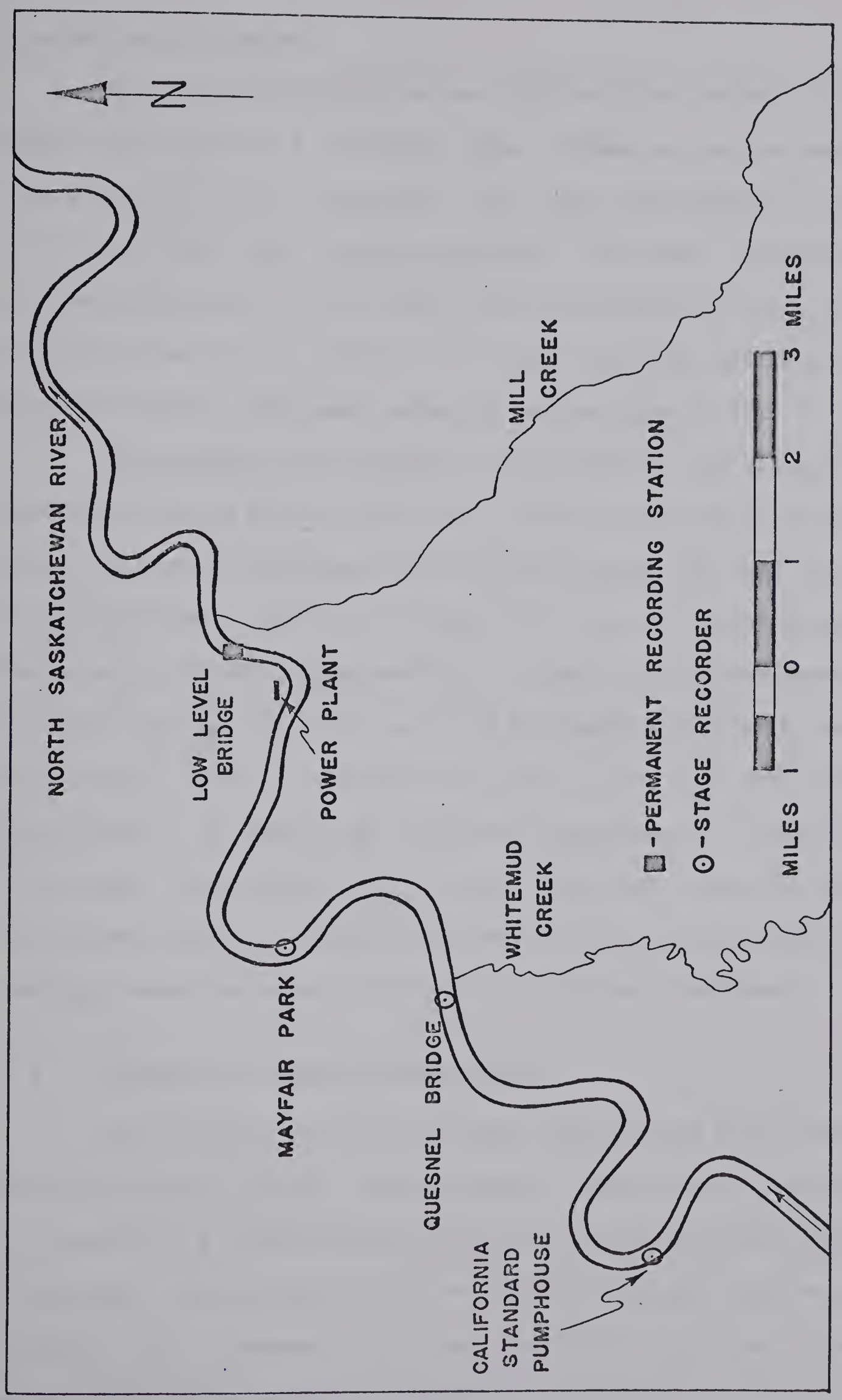


FIGURE 3-1 MAP OF THE NORTH SASKATCHEWAN RIVER THROUGH EDMONTON

drawdown were discarded.

The mean daily discharges were obtained from the Water Survey of Canada which operates a continuous stage recorder at the Low Level Bridge (See Figure 3-1 for the location). This gauge was situated in a section of the river which was free from ice cover. Warm water, which had been used as cooling water for the power plant, discharged into the river keeping it free of ice. With no ice cover, the discharges were simply obtained from the open water rating curve (see Appendix A).

The velocity distribution in a cross-section was measured at the Mayfair Park gauge during mid-winter. For the insertion of the current meter, six inch diameter holes were drilled through the ice. Velocity distributions were taken every 50 feet with some additional measurements taken near each bank (see Appendix A). A small Ott current meter, which included a counter and timer, was used for taking the velocity measurements. At each hole, velocity readings were taken at every 0.25 feet for the entire depth. In addition to the velocity measurements at each hole; the river depth, ice thickness and the water level with respect to the ice surface were noted. The above measurements, with the exception of velocity readings, were also made at the California Standard Pumphouse.

## 3.3 Treatment of Stage-Discharge Data

The ice cover period on the North Saskatchewan River lasted approximately four months; from November 21, 1969 to March 21, 1970. In Figure 3-2, a stage-discharge relation was plotted for the Mayfair Park gauge. Rating curves for three different ice cover periods were obtained: (i) freeze-up (ii) break-up (iii) mid-winter. The open water curve is also shown on this plot.

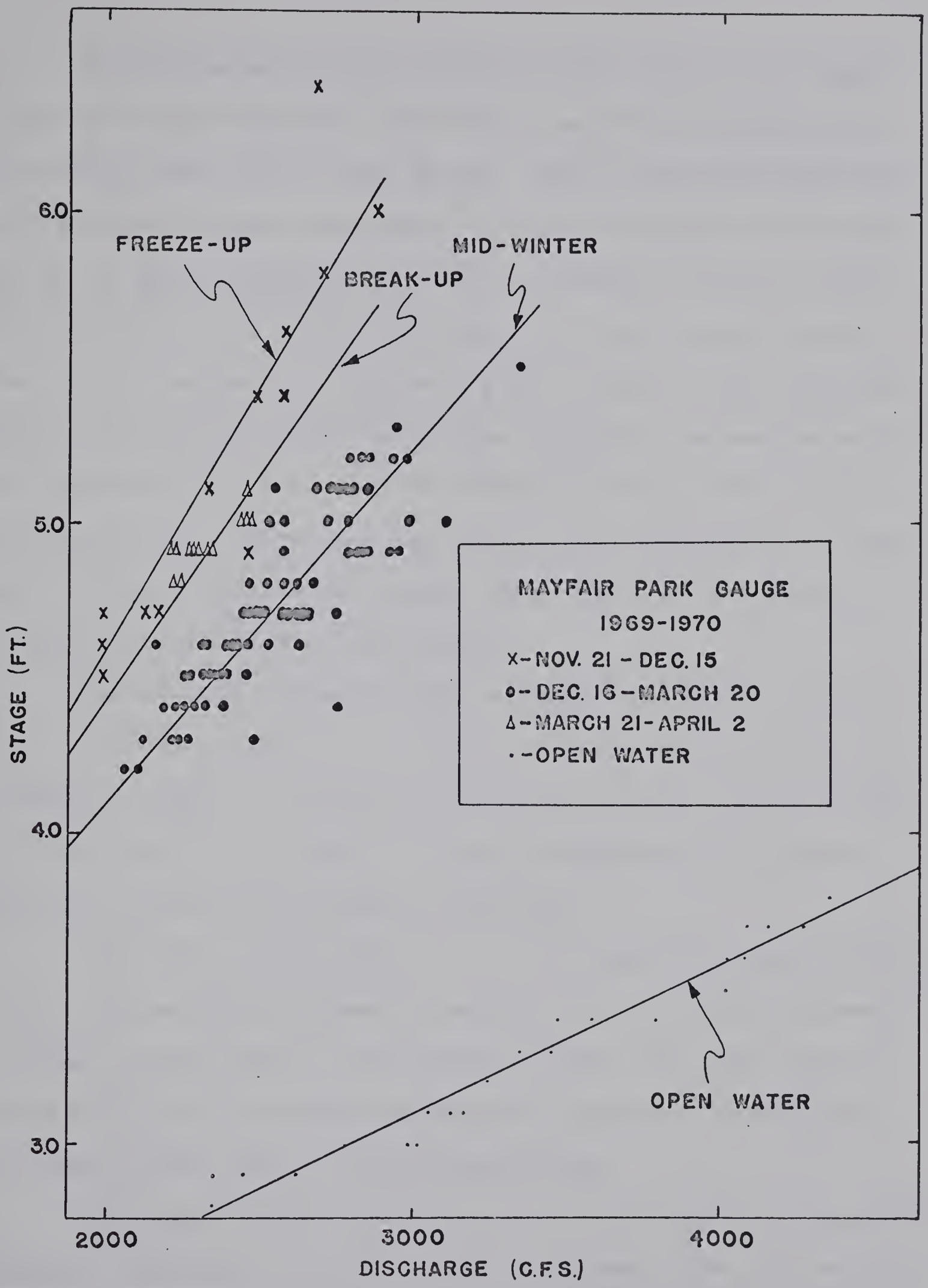


FIGURE 3-2 STAGE-DISCHARGE CURVES

Of the three periods, the freeze-up period requires the highest stage for a given discharge. The freeze-up period was preceeded by an ice jam just below the Low Level Bridge. The ice jam induced additional errors to the discharge measurements by causing increases in the stage due to ice debris floating in the river, a backwater from the ice jam and a decrease in the width of the river. As time progressed during the freeze-up period, the stage for a given discharge rapidly decreases. This was due to the "washing out" of the ice jam and the smoothening of the underside of the ice. The ice thickness increases rapidly during this period but it can be seen from the plot that the decrease in stage due to the smoothening of the ice more than offsets the increase in stage due to the increased ice thickness.

The mid-winter stage-discharge relationship is stable. During this period the ice grows very little in thickness and the decrease in roughness is small. This period continues for the major portion of the ice cover period as it lasts for all but the approximate three week period of freeze-up and one week of break-up.

The break-up period sees a rise in the stage for a given discharge. During this period the thinnest ice sections of the river and the small tributary streams break up. This broken ice then flows under the main sheet of ice, thus increasing the effective roughness. The additional frictional losses result in the increased stage.

The stage-discharge curve for an ice covered channel is a variable feature. The changes in roughness and ice thickness cause this variation. Ice jams do not occur as regular as the above causes but their effect can be very large due to changes in channel width and backwater effects.

The length, of the three periods previously discussed, varys from year to year depending on the climatic conditions. A measurement must be made during each period to determine the stage-discharge relationship for ice cover.

## 3.4 Treatment of Velocity Data.

The velocity distribution was measured at the Mayfair Park gauge on February 7, 1970. The ice was approximately 2 1/2 months old with an average thickness of 1 1/2 feet. The measured velocity distribution is shown in Figure 3-3.

The velocity distribution measurements are treated according to the theoretical approach using the Prandtl - Karman law. Measurements were made on 12 verticals and a regression analysis was utilized to obtain the best fit straight line through the points. The equivalent roughness height, $k_s$, was then found and related to Manning's n according to equation (2.12). Once the Manning coefficient was obtained for both the bed and the ice boundaries, a composite value was calculated by the methods mentioned in the previous chapter. The calculated data are tabulated and explained in Appendix B. The values obtained for the composite n are:

| | |
|---|---|
| Larsen | 0.0219 |
| Weighted Average | 0.0225 |
| Belokan and Sabaneer | 0.0231 |
| Pavlovskiy | 0.0238 |

The ice cover was found to be smooth with a Manning coefficient of 0.0150. From observations made, the ice taken from the channel appeared to be completely smooth. This is contrary to what was observed

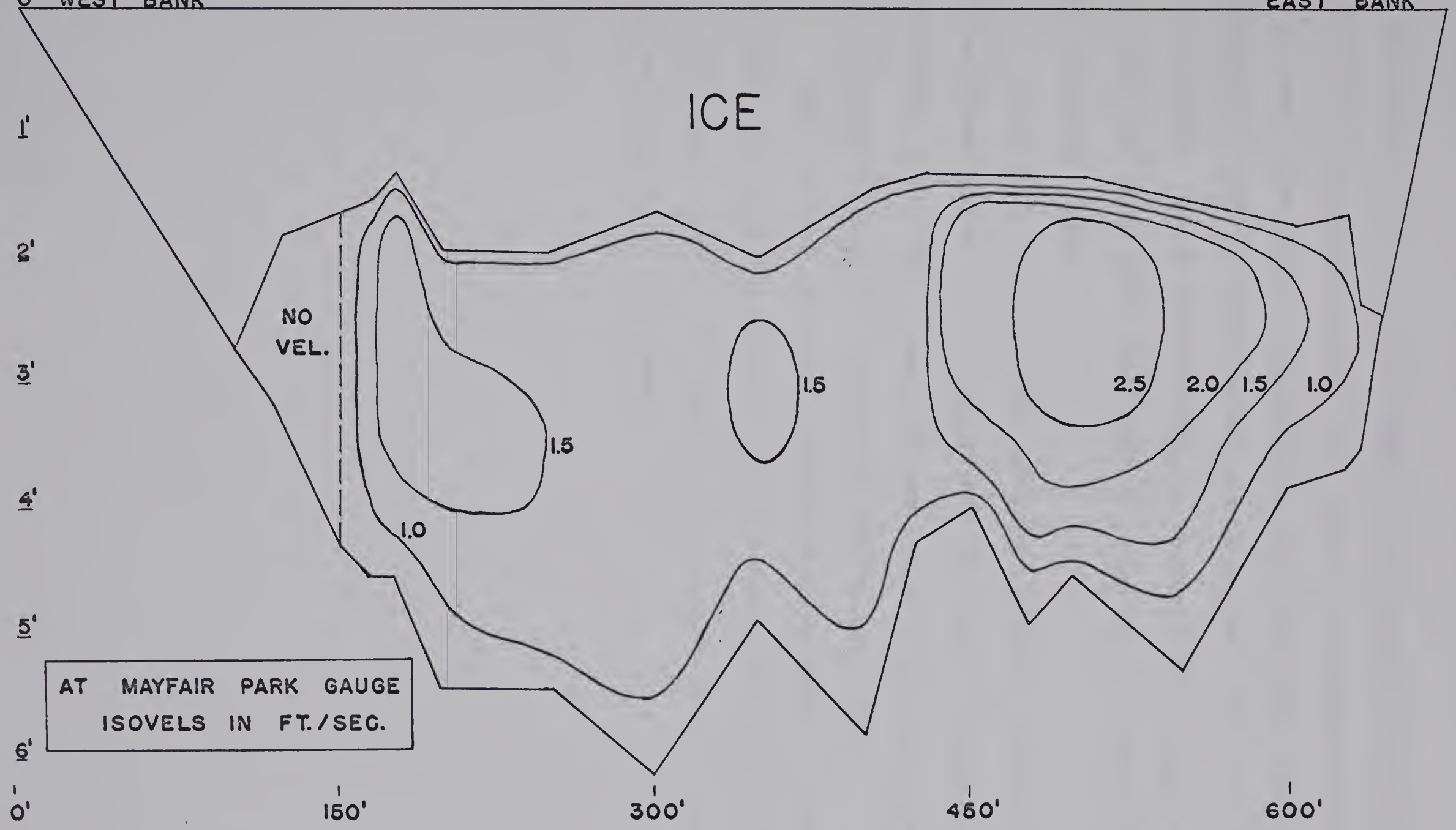


FIGURE 3-3 CROSS-SECTION OF THE NORTH SASKATCHEWAN RIVER

by both Carey (1967) and Larsen (1969). The ripplelike configurations observed by Carey were very small and they did not become noticeable until late in the winter. The author believes that these ripplelike and dunelike features may be caused by a phenomenon similar to that of sand dunes. The observations made on the North Saskatchewan were in the plain bed region while those made by Larsen were in the dune phase due to greater depths.

It should be noted that the values of equivalent roughness of the bed showed rather large fluctuations. This would be expected since the bed was mostly small gravel with some rather large rocks spread on top. The roughness of the ice was considerably more regular.

The flow depth in an ice covered channel is greatly increased over that of an open channel due to the increase in the wetted perimeter. The percentage increase will depend on the roughness of the ice and the original roughness of the channel.

# CHAPTER IV

# SURGES

## 4.1 General

This chapter briefly discusses the previous work done on surges as well as the theoretical aspects of the problem. Open channel surges are considered first and then modifications are made to include the ice cover condition. The theory is so developed that it can be easily adapted to the computer.

## 4.2 Literature Review

In reviewing the literature there has recently been a considerable increase of interest in surges. This is a result of the advent of the digital computer which has enabled these problems to be solved more rapidly. Most of the studies have been concerned with changes in the flow rate and tidal effects on open channels. The effect on surges caused by an ice cover on open channel has only been briefly mentioned.

Grushevskiy, (1965) discusses the characteristics and peculiarities of the various types of unsteady movement of water in unerodable natural channels. He describes the propagation of surges under varying channel conditions. In mentioning ice cover he states that the celerity and height of surges are decreased under these conditions. There are no specific conclusions reached in his paper as it is a general description of unsteady flow.

Cooper (1966) performed some laboratory experiments on the effect of a surface cover on open channel surges. Using surface covers of vary-

ing rigidity, roughness and weight, he observed surges propagating through initially still water. From his experiments he found that the addition of a surface cover reduces the velocity and height of surges. The decreases he observed in laboratory models were not as great as those in the field.

To compute surge propagation against an adverse current, Collins and Fersht (1968) developed a numerical scheme for the integration of the basic non-linear equation with friction. They used a mixed technique involving finite difference forms combined with a fourth-order Runge-Kutta method. They checked their procedure against observations made during a hurricane. The computed results give a reasonably good representation of the actual observations.

In 1968, Baltzer and Chintu Lai simulated unsteady flows in rivers using three different methods. They used the method of characteristics, the power series method and the implicit finite difference method, all of which are suited for computer execution. Comparisons of simulated flows obtained by using each of these methods with numerous field measurements indicate generally good agreement.

In demonstrating the use of the digital computer for the simulation of prismatic open-channel wave problems, Martin and De Fazio (1969) used the finite-difference technique. Varying boundary conditions were imposed on the channels to simulate different engineering situations. The comparison of the computer solutions and experimental values indicates close agreement especially on the maximum values of water-surface elevation.

A tidal study was carried out on the St. Lawrence River in 1970 by Kamphuis. He also applied the finite-difference technique to solve the equations of continuity and motion. He suggests that where the cross-

sections vary considerably with distance the accuracy of the solution is much improved if shorter section lengths are used. The computer solutions were similar to the field observations.

The previous work on surges has mainly considered open channel surges. There has been very little work done on surges under an ice cover and it has produced only limited success. The computer simulations of open channel surges have provided rather good results. Although several conditions have been imposed on the channels, there has been no previous attempt to simulate surges under an ice covered channel.

## 4.3 Theoretical Aspects of Surges

Changing the rate of flow causes a surge to form and propagate downstream in a channel. The properties of the surge are dependent upon the properties of the flow and the channel. The one-dimensional equations of continuity and linear momentum provide the necessary tools for analyzing these surges. The two equations allow the flow characteristics of the channel to be completely expressed in terms of two variables, e.g., depth and velocity.

From the definition sketch in Figure 4.1, H is the stage, y is the depth of flow, z is the channel bottom elevation, V is the average cross-sectional velocity, A is the cross-sectional area of flow, B is the top width of flow, and P is the wetted perimeter of the open channel. If x is the horizontal co-ordinate and t, time, the continuity equation may be written as:

$$\frac{\partial}{\partial x}(VA)\,dx = -B\,dx\,\frac{\partial H}{\partial t} \qquad \text{- - - - - - - - - - - - - - - - - (4.1)}$$

Simplifying gives:

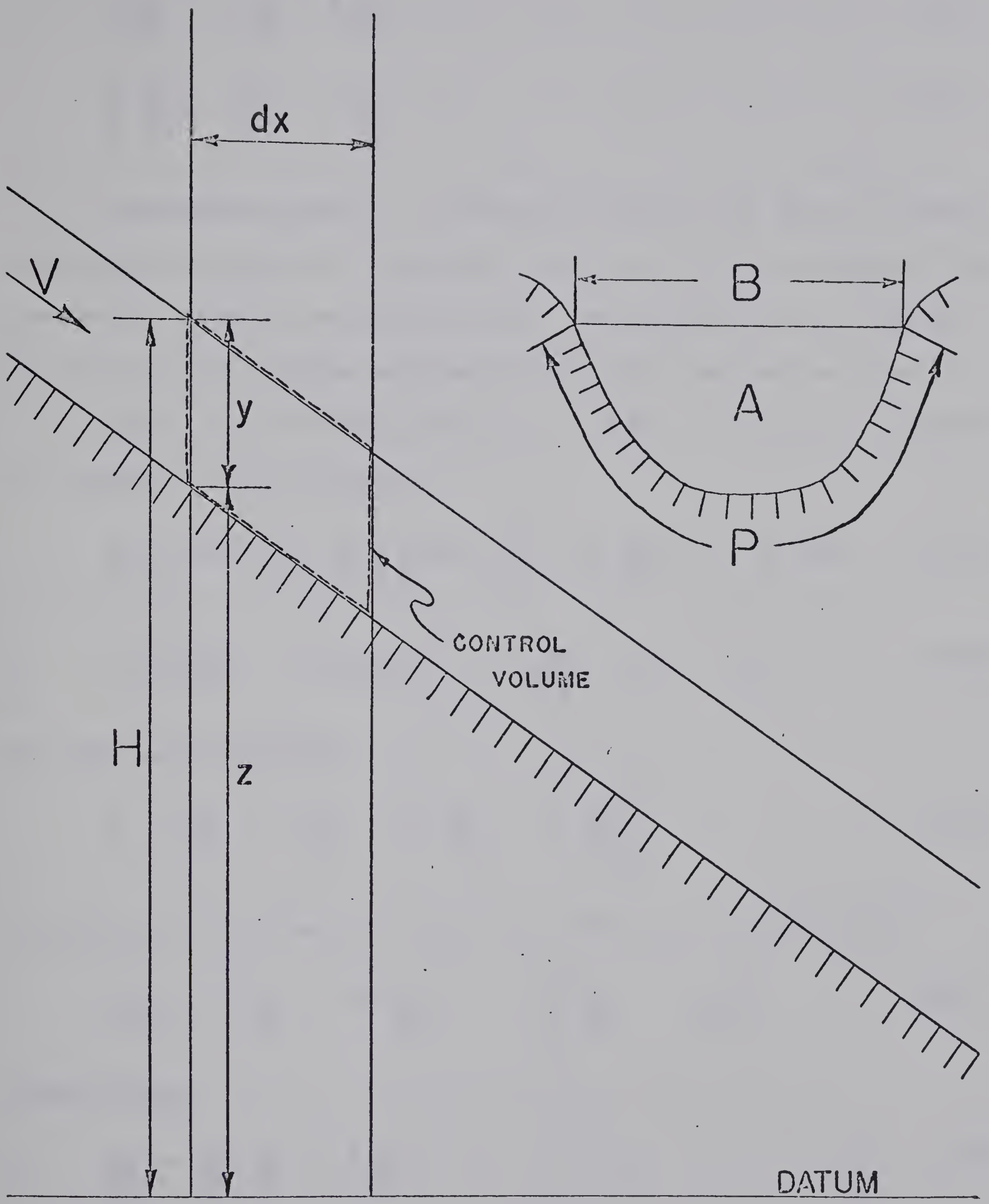


FIGURE 4-1 DEFINITION SKETCH

$$B\frac{\partial H}{\partial t} + V\frac{\partial A}{\partial x} + A\frac{\partial V}{\partial x} = 0 \qquad \text{- - - - - - - - - - - - - - - - - (4.2)}$$

$$\frac{A}{B}\frac{\partial V}{\partial x} + \frac{\partial H}{\partial t} + V\frac{\partial y}{\partial x} = 0 \qquad \text{- - - - - - - - - - - - - - - - - (4.3)}$$

The momentum equation is obtained by equating the rate of increase of momentum in the control volume plus the rate of efflux of momentum from the control volume to the applied force. The applied force is a sum of the pressure force and the bed shear force, where the pressure force is $-\gamma A\ (\partial H/\partial x)\ dx$ and the shear force is $-\tau\, Pdx = -\gamma A\, S_f\, dx$. The momentum equation is thus written as,

$$\frac{\partial}{\partial t}\left(\frac{\gamma}{g}\, dx AV\right) + \frac{\partial}{\partial x}\left(\frac{\gamma}{g}\, dx AV\cdot V\right) = -\gamma A\frac{\partial H}{\partial x}\, dx - \gamma A\, S_f dx \qquad \text{- - (4.4)}$$

$$\frac{1}{A}\left[\frac{\partial (AV)}{\partial t} + \frac{\partial (AV\cdot V)}{\partial x}\right] = -g\frac{\partial H}{\partial x} - g\, S_f \qquad \text{- - - - - - - - (4.5)}$$

The left hand side becomes

$$\frac{1}{A}\left[A\frac{\partial V}{\partial t} + V\frac{\partial A}{\partial t} + 2AV\frac{\partial V}{\partial x} + V^2\frac{\partial A}{\partial x}\right] \qquad \text{- - - - - - - - - (4.6)}$$

Using equation (4.2) and multiplying the left hand side by A, gives

$$A\frac{\partial V}{\partial t} + V\frac{\partial A}{\partial t} + 2AV\frac{\partial V}{\partial x} + V\left[-A\frac{\partial V}{\partial x} - B\frac{\partial H}{\partial t}\right] \qquad \text{- - - -- -(4.7)}$$

Substituting:

$$\frac{\partial A}{\partial t} = \frac{\partial A}{\partial H}\frac{\partial H}{\partial t} = B\frac{\partial H}{\partial t} \qquad \text{- - - - - - - - - - - - - - - - - - - (4.8)}$$

Expression (4.7) becomes

$$A\frac{\partial V}{\partial t} + VB\frac{\partial H}{\partial t} + 2AV\frac{\partial V}{\partial x} - AV\frac{\partial V}{\partial x} - VB\frac{\partial H}{\partial t} \qquad \text{- - - - - - - (4.9)}$$

which reduces to:

$$A \frac{\partial V}{\partial t} + AV \frac{\partial V}{\partial x} \qquad \text{- - - - - - - - - - - - - - - - - - - - - (4.10)}$$

Now divide expression (4.10) by A to revert back to the left hand side of equation (4.5),

$$\frac{\partial V}{\partial t} + V \frac{\partial V}{\partial x} \qquad \text{- - - - - - - - - - - - - - - - - - - - (4.11)}$$

Thus the momentum equation reduces to,

$$\frac{\partial V}{\partial t} + V \frac{\partial V}{\partial x} + g \frac{\partial H}{\partial x} + g S_f = 0 \qquad \text{- - - - - - - - - - (4.12)}$$

Since the right hand sides of the continuity and momentum equations are equal to zero they can be equated by using $\lambda$, a multiplying constant:

$$\frac{\partial V}{\partial t} + V \frac{\partial V}{\partial x} + g \frac{\partial H}{\partial x} + gS_f + \lambda \left[ \frac{A}{B} \frac{\partial V}{\partial x} + \frac{\partial H}{\partial t} + V \frac{\partial y}{\partial x} \right] = 0 \quad \text{- (4.13)}$$

In order to eliminate H, it should be noted that:

$$H = z + y \qquad \text{- - - - - - - - - - - - - - - - - - - - (4.14)}$$

$$\frac{\partial H}{\partial x} = \frac{\partial z}{\partial x} + \frac{\partial y}{\partial x} \qquad \text{- - - - - - - - - - - - - - - - - - - - (4.15)}$$

$$\frac{\partial H}{\partial t} = \frac{\partial y}{\partial t} \qquad \text{- - - - - - - - - - - - - - - - - - - - (4.16)}$$

Substituting for $\partial H/\partial x$ and $\partial H/\partial t$ in equation (4.7) gives:

$$\frac{\partial V}{\partial t} + V \frac{\partial V}{\partial x} - gSo + g \frac{\partial y}{\partial x} + gS_f + \lambda \left[ \frac{A}{B} \frac{\partial V}{\partial x} + \frac{\partial y}{\partial t} + V \frac{\partial y}{\partial x} \right] \quad \text{- - (4.17)}$$

where: $So = -\partial z/\partial x$ - - - - - - - - - - - - - - - - - - - - (4.18)

Rearranging equation (4.17) gives:

$$\frac{\partial V}{\partial t} + \left(V + \lambda \frac{A}{B}\right) \frac{\partial V}{\partial x} + \lambda\left[\frac{\partial y}{\partial t} + \left(V + g/\lambda\right) \frac{\partial y}{\partial x}\right] + g(S_f - So) \quad - - - \quad (4.19)$$

Now find $\lambda$ to make

$$V + \lambda \frac{A}{B} = V + g/\lambda \quad - - - - - - - - - - - - - - - - \quad (4.20)$$

which is $\lambda = \pm \sqrt{\frac{gB}{A}}$ $\quad - - - - - - - - - - - - - - - - \quad (4.21)$

The terms containing $\partial V/\partial t$, $\partial V/\partial x$, $\partial y/\partial t$, $\partial y/\partial x$ become total derivatives if:

$$\frac{dx}{dt} = V + \lambda \frac{A}{B} = V + g/\lambda \quad - - - - - - - - - - - - - - - - \quad (4.22)$$

$$\frac{dx}{dt} = V \pm \sqrt{\frac{gA}{B}} = V \pm Co \quad - - - - - - - - - - - - - - - - \quad (4.23)$$

where $\pm Co = \pm \sqrt{\frac{gA}{B}}$ $\quad - - - - - - - - - - - - - - - - - - \quad (4.24)$

Therefore, along a positive characteristic where:

$$\lambda = + \sqrt{\frac{gB}{A}} \quad \text{and} \quad \frac{dx}{dt} = V + Co^{+} \quad - - - - - - - - - \quad (4.25)$$

equation (4.19) becomes:

$$\frac{Co^{+}}{g} \frac{dV}{dz} + \frac{dy}{dt} + Co^{+} (S_f - So) = 0 \quad - - - - - - - - - \quad (4.26)$$

Similarly along a negative characteristic where:

$$\lambda = - \sqrt{\frac{gB}{A}} \quad \text{and} \quad \frac{dx}{dt} = V - Co^{-} \quad - - - - - - - - - - - \quad (4.27)$$

equation (4.19) becomes:

$$\frac{Co^{-}}{g} \frac{dV}{dt} - \frac{dy}{dt} + Co^{-} (S_f - So) = 0 \quad - - - - - - - - - - - \quad (4.28)$$

Figure 4-2 shows the characteristic grid on the x-t plane used in solving the differential equations. With subcritical flow, a disturbance is propagated both upstream and downstream from the point of occurence, whereas in supercritical flow the disturbances only propagate downstream. This can be seen graphically in Figures 4-3 and 4-4 where a change in conditions at point L effects all the shaded area.

## 4.4 Variations For Ice Conditions

The hydraulic characteristics of an open channel are radically changed with the imposition of an ice cover. The flow in an ice covered river is in some ways similar to the flow in a conduit. In a wide river there is one important difference and that is, that the cross-sectional area will adjust according to the need because the ice is floating on the water.

The ice cover produces a substantial increase in the wetted perimeter, see Figure 4-5. Assuming a thin cover on a wide channel, the hydraulic radius is reduced to near half the value of the open channel radius. Also making the assumption that the flow is uniform and keeping the flow rate constant, the variation in depth is computed from Manning's equation as indicated below. For an open channel

$$Q = \frac{1.49}{n_2} d^{2/3} S^{1/2} bd \qquad \text{- - - - - - - - - - - - - - - - - (4.29)}$$

For an ice covered channel

$$Q = \frac{1.49}{n} \left(\frac{d_1}{2}\right)^{2/3} S^{1/2} bd_1 \qquad \text{- - - - - - - - - - - - - - (4.30)}$$

Equating the two equations gives:

$$n_2 d_1^{5/3} = n \cdot 2^{2/3} \cdot d^{2/3} \qquad \text{- - - - - - - - - - - - - - - - (4.31)}$$

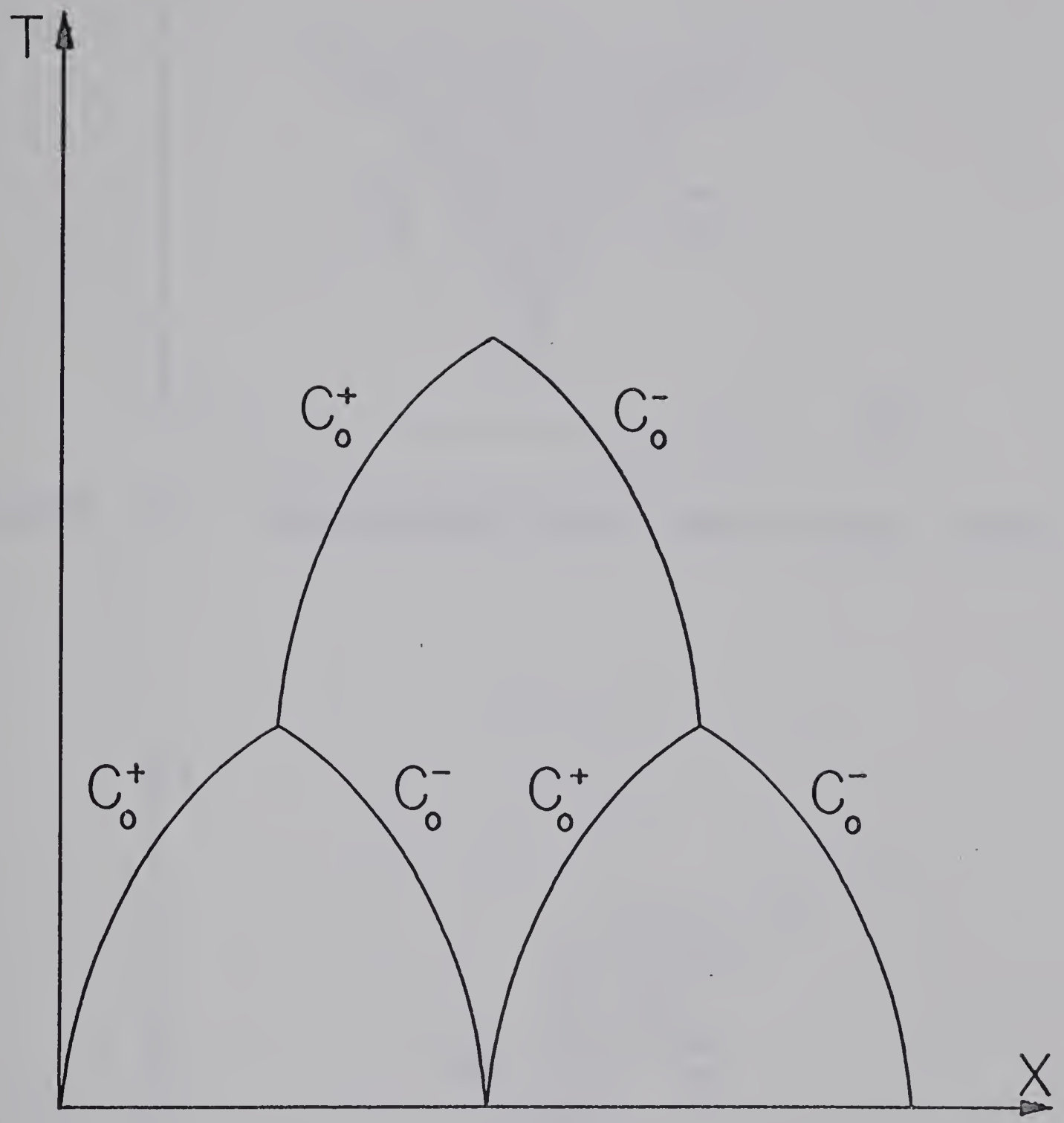


FIGURE 4-2 GRID OF CHARACTERISTICS IN X-T PLANE

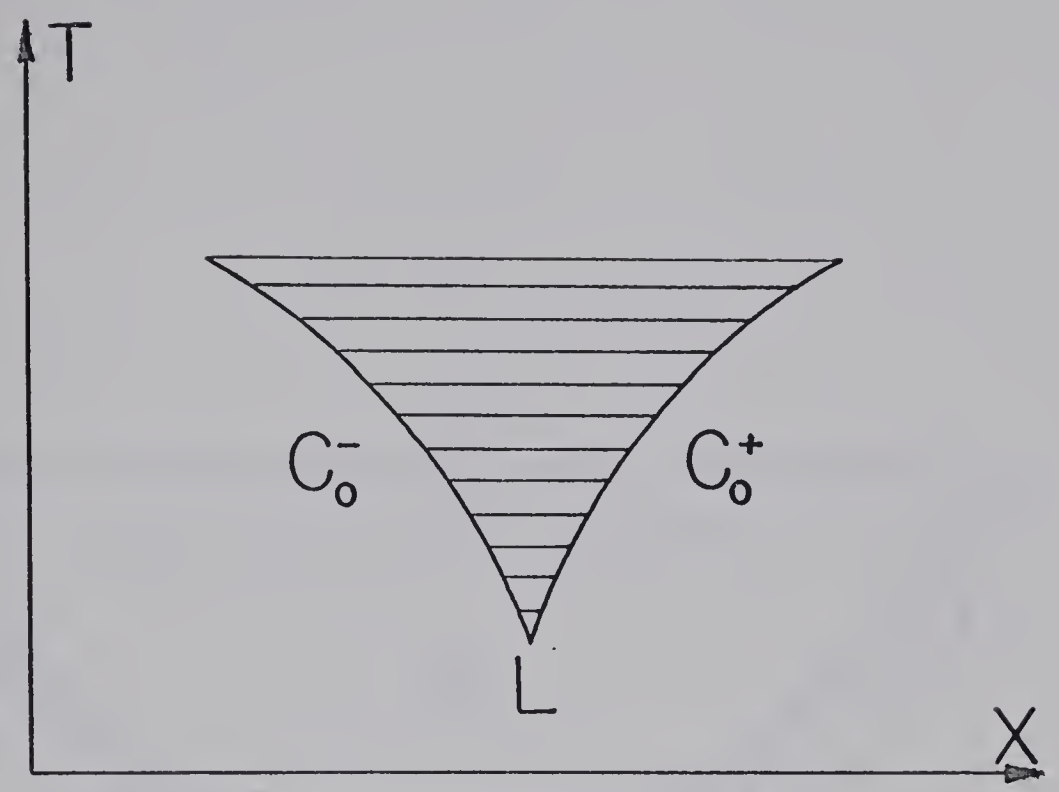


FIGURE 4-3 CHARACTERISTICS IN SUBCRITICAL FLOW

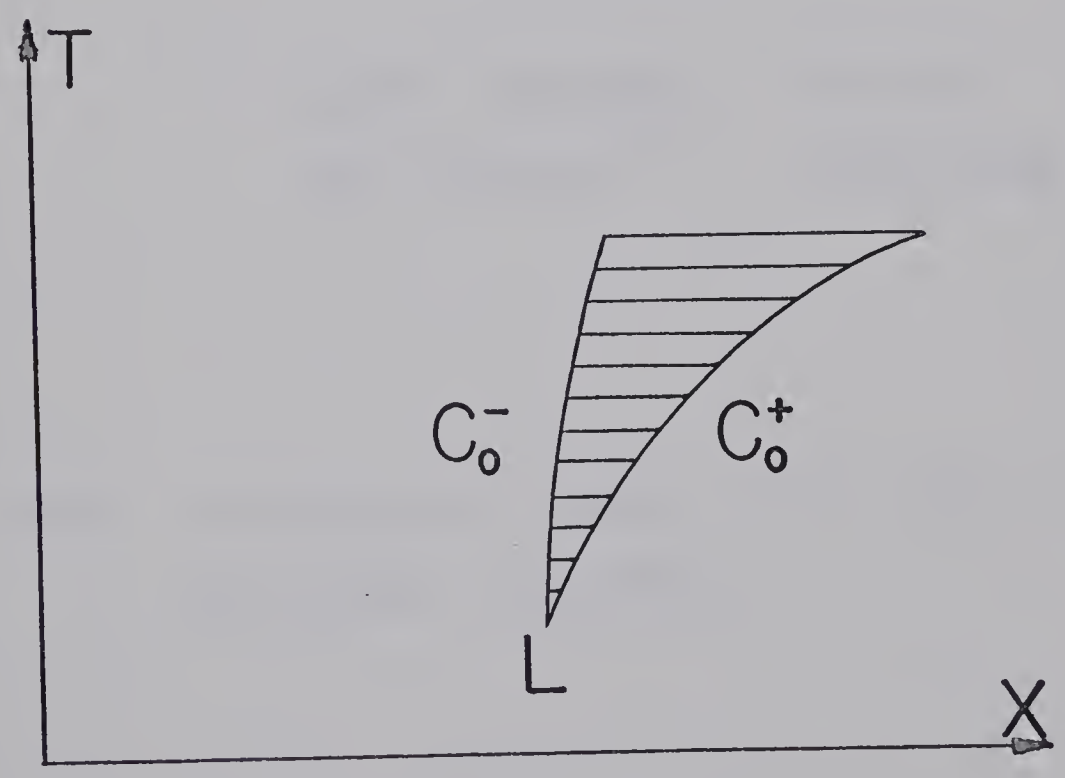


FIGURE 4-4 CHARACTERISTICS IN SUPERCRITICAL FLOW

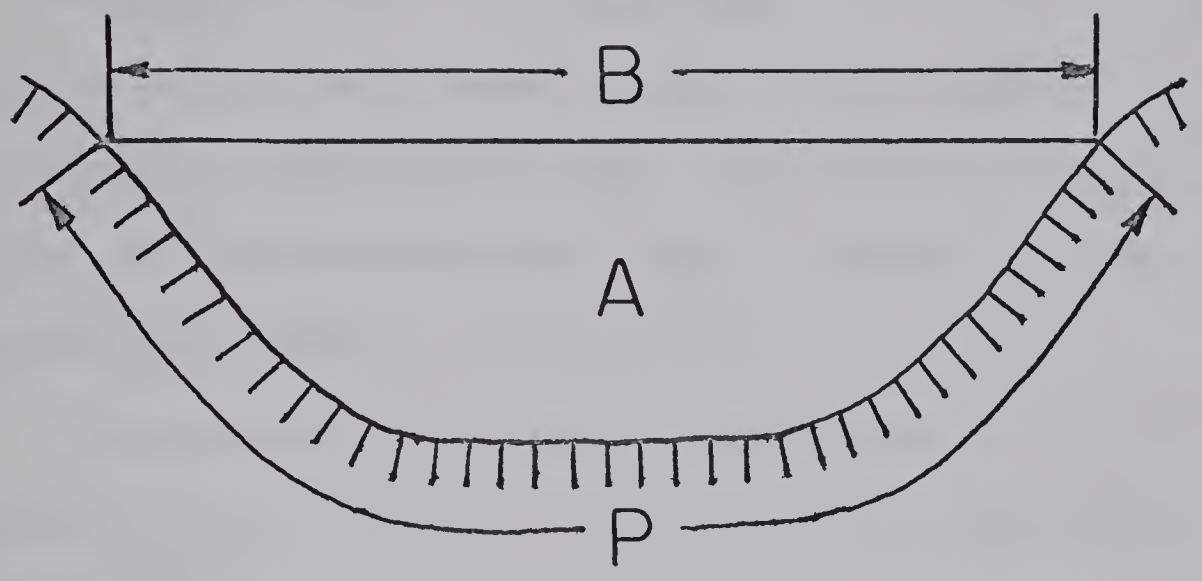


HYDRAULIC RADIUS

OPEN CHANNEL $R=A/P$

ICE COVER $R=A/P+B$

FIGURE 4-5 HYDRAULIC RADIUS FOR OPEN AND ICE COVERED CHANNELS

$$d_1 = 1.32 \left(\frac{n}{n_2}\right)^{3/5} d \qquad \text{- - - - - - - - - - - - - - - - - - - (4.32)}$$

If the ice roughness was equal to the bottom roughness, the increase in flow depth with an ice cover would be 32%. The ice is generally smoother than the bed, therefore a more practical value would be to assume the ice roughness coefficient n equal to half the bed roughness coefficient; thus the increase in depth would be 12%. For more exact results, a roughness based on both boundaries are outlined in Chapter II should be applied to determine the changes in depth of flow.

The above modifications were applied when solving the characteristic equations for ice cover conditions. Any other effects due to the ice cover were neglected.

## 4.5 Computer Solution to Differential Equations

For the solution of the differential equations, the initial conditions must be known as well as the boundary conditions at either end of the channel. From Figure 4-6, the conditions of time, velocity, depth, and distance are known at points L and M. It is required to obtain the conditions mentioned above for point N. Thus, along a positive characteristic, equations (4.25) and (4.26) become:

$$\frac{T_N - T_L}{X_N - X_L} = \frac{1}{V + Co^+} \qquad \text{- - - - - - - - - - - - - - - - - - - (4.33)}$$

$$\frac{Co^+}{g}\left(\frac{V_N - V_L}{T_N - T_L}\right) + \left(\frac{Y_N - Y_L}{T_N - T_L}\right) + Co^+ (S_f - So) = 0 \qquad \text{- - - (4.34)}$$

And similarly along the negative characteristic, equations (4.27) and (4.28) become:

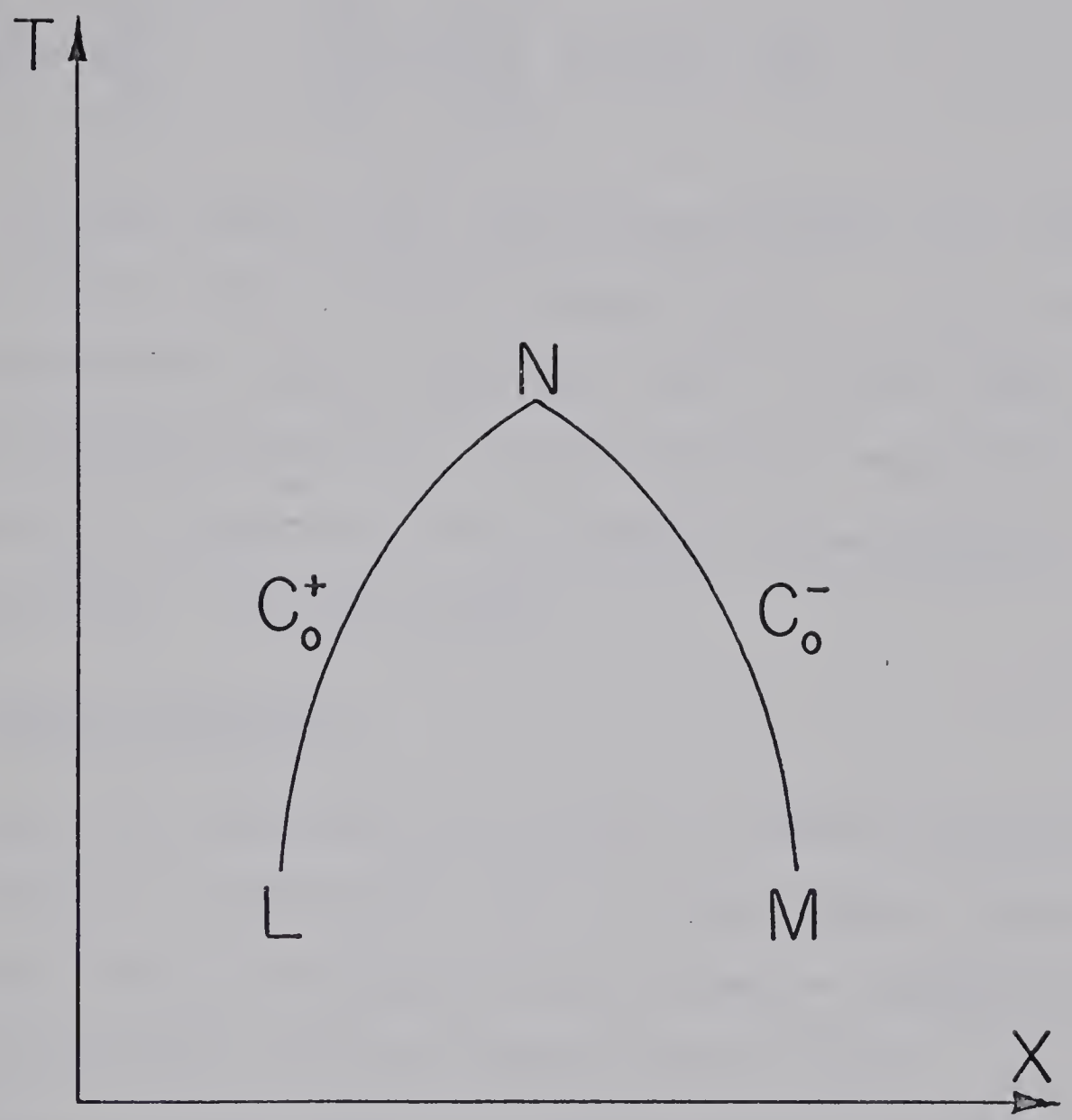


FIGURE 4-6 DEFINITION SKETCH

$$\frac{T_N - T_M}{X_N - X_M} = \frac{1}{V - Co^-} \qquad \text{- - - - - - - - - - - - - - - - - - - (4.35)}$$

$$\frac{Co^-}{g}\left(\frac{V_N - V_M}{T_N - T_M}\right) - \left(\frac{Y_N - Y_M}{T_N - T_M}\right) + Co^-(S_f - So) \qquad \text{- - - - - - - - - (4.36)}$$

The values used for $Co^{\pm}$ and V are an average of the values of $Co^{\pm}$ and V at points L and M. The four unknowns ($Y_N$, $V_N$, $T_N$, $X_N$) at point N can be obtained from the four equations. This is a quasi-linear problem since the coefficients $Co^{\pm}$, $Co^-$, $V + Co^+$ and $V-Co^-$ depend on the values of $Y_N$ and $V_N$. The solution to these equations can be obtained by implementing the predictor - corrector process.

## 4.6 Boundary Conditions

The initial condition of the channel is imposed on the x-axis of the x-t diagram. Generally the initial condition imposed is that of a steady-flow condition, although any condition may be imposed if the velocities and depths are known along the entire x-axis.

The t-axis at one end of the channel and the line parallel to the t-axis at the other end of the channel are the lines on which the boundary conditions are imposed. One of the two dependent variables must be specified as a boundary condition. At the boundaries only one characteristic leads to the unknown as shown in Figures 4-7 and 4-8. This results in two differential equations available for the solution of the condition at the boundaries. Since either depth or velocity is an imposed condition at the boundaries and the distance is known, the two available equations provide the means for obtaining the two unknowns.

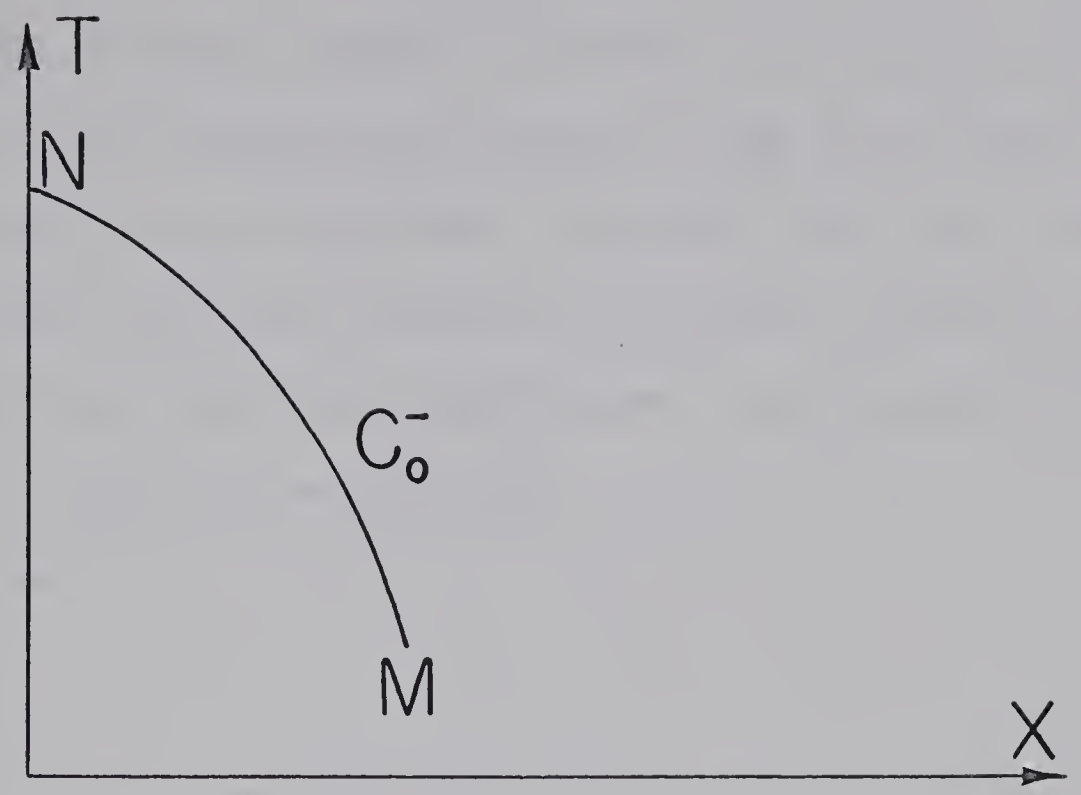


FIGURE 4-7 LEFT HAND BOUNDARY

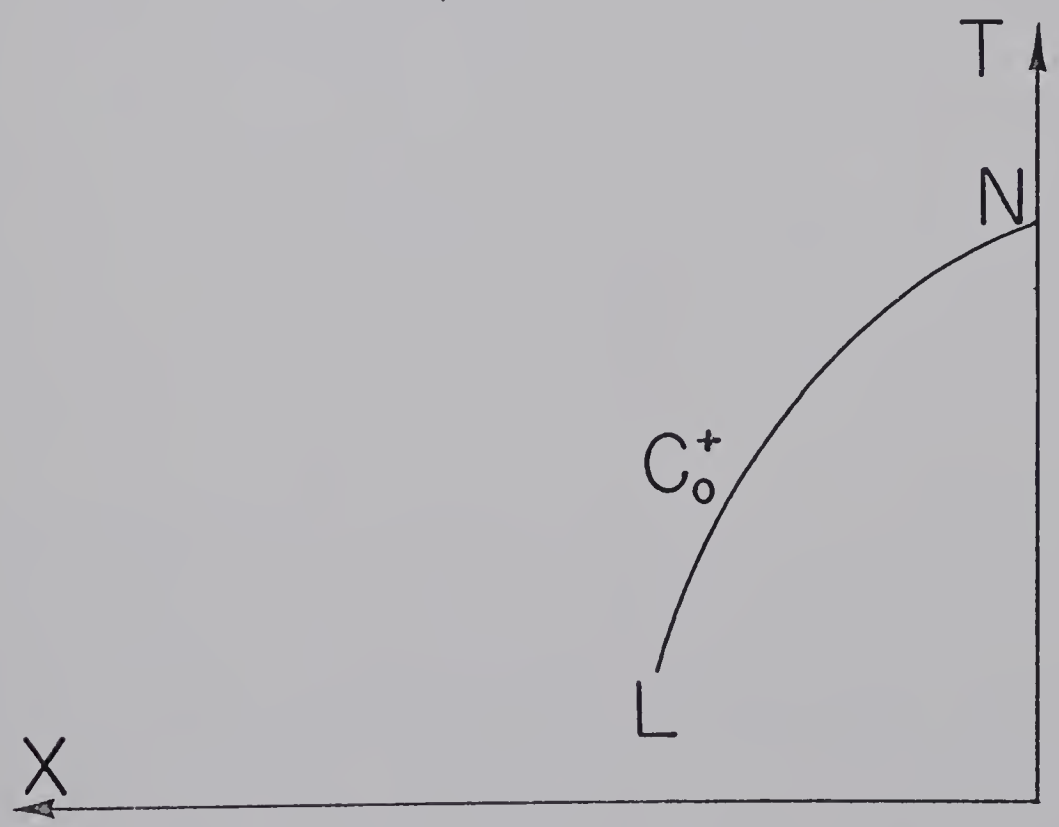


FIGURE 4-8 RIGHT HAND BOUNDARY

Several different boundary conditions may be imposed on a channel to simulate various engineering situations. Some of the more typical boundary conditions are hydrographs, reservoirs, dead ends, free-fall and junctions. With the initial condition and boundary conditions imposed on every channel that comprises a total system, the propagation of surges through the channels can be simulated.

# CHAPTER V

# THE SIMULATION OF SURGES

## 5.1 General

A computer program, based on the theory expressed in the previous chapter, was written for surge propagation through a channel. This program was tested against observations made on the Brazeau and North Saskatchewan River in Alberta. The periodic releases of large quantities of water from the Brazeau Reservoir caused surges to form and propagate down the channels. Various recording stations along these channels provided information on the surge heights and speeds.

Surges of various sizes and frequency were imposed at the upstream end of the simulated channel and were allowed to propagate through the channel under various conditions. Computer runs were made on both open channel and ice cover conditions with the solutions being provided in the form of plots. The velocities and depths in the channel were plotted against distance at various times and against time at various stations along the channel.

## 5.2 Field Observations

In order to test the accuracy of the computer solutions, it was necessary to obtain some field data on surge propagation. The required data was obtained from the North Saskatchewan River where the stage-recorders on the river record the propagation of the surges, which are formed from the controlled releases of water at the Brazeau Reservoir.

Figure 5-1 gives a plan of the section of the North Saskatchewan and Brazeau Rivers used for observations. There are stage recorders located at Rocky Mountain House, Lodgepole, Drayton Valley and Edmonton on the North Saskatchewan River. The gauge at Drayton Valley, which is operated by Calgary Power, gave very poor readings as the river cross-section was not stable; this resulted in the discarding of those readings. The gauges at Edmonton and Rocky Mountain House, which are operated by the Water Survey of Canada, record the stage continuously through the entire year. The river at the Low Level Bridge gauge at Edmonton is ice free for the entire year whereas an ice cover forms during the winter on the river at Rocky Mountain House. The cross-section, recorder, charts and rating curves were obtained from the Water Survey of Canada for the periods, September, 1967 to March, 1968 and May, 1969 to May, 1970. The gauge at Lodgepole, which only records during the summer months, was a recent installation; therefore, the information as mentioned above was available only for the period May, 1969 to October, 1969.

On the Brazeau River there is a stage recorder located just below the Big Bend Plant on a section of the river which is ice free all year. Since recent readings were not accurate, due to the shifting of the cross-section, Calgary Power supplied recorder charts and rating curves for the period September, 1967 to March, 1968. The data obtained from this gauge provided very good information on the variation in discharges due to the releases of large quantities of water through the turbines at the Big Bend Plant.

The cross-sections of the North Saskatchewan River at the recording stations were found to increase slightly in width as one progressed down-

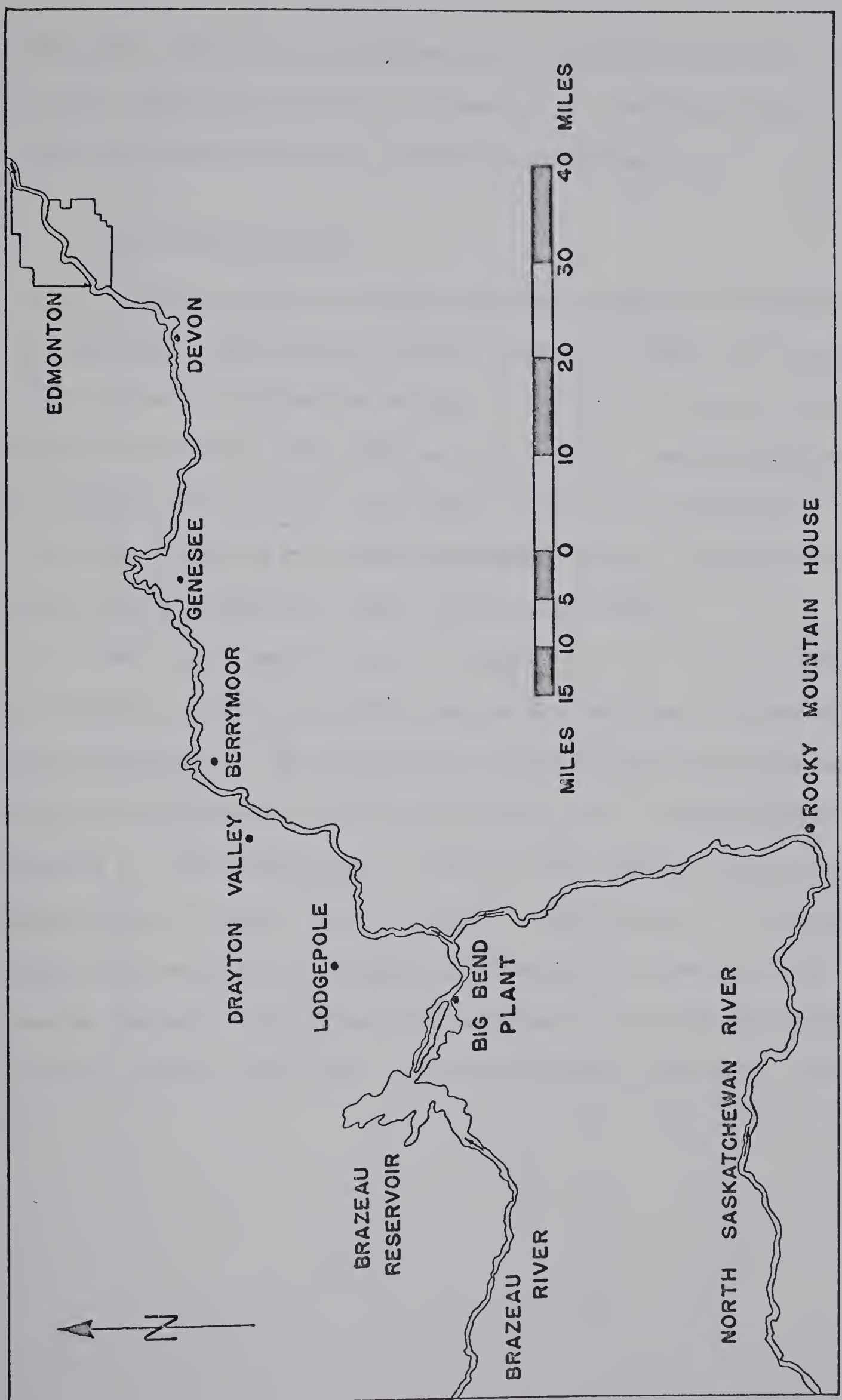


FIGURE 5-1 MAP OF THE NORTH SASKATCHEWAN AND BRAZEAU RIVERS

stream, but they could be approximated by trapezoidal sections. Similarly, from the longitudinal profile in Figure 5-2, it can be seen that the bed slope slowly decreases as one progresses downstream.

## 5.3 The Computer Program

Since the solution of surge problems are readily obtained by numerical techniques, the high-speed digital computer is very well suited for the task. A computer program was written in Fortran IV language using the equations developed in the previous chapter with a separate program written for plotting the results. The computer analysis was carried out at the University of Alberta on an IBM System/360, Model 67, computer with the results being plotted by a model 663 Cal Comp Plotter.

The program was written as a number of subroutines so as to increase its flexibility and to allow for the ease in making any changes which might be necessary. The tabulation in Table 5.1 gives the name and purpose of the subroutines with a complete listing of program available in Appendix C. The subroutines, as listed in the appendix, are set up to handle surges in an ice covered channel. Modifications in the subroutines REACH, BDY1 and BDY2 were required in changing from open water to ice covered channels. The changes made were due to the different hydraulic radii for the two conditions. This was previously discussed in Chapter IV.

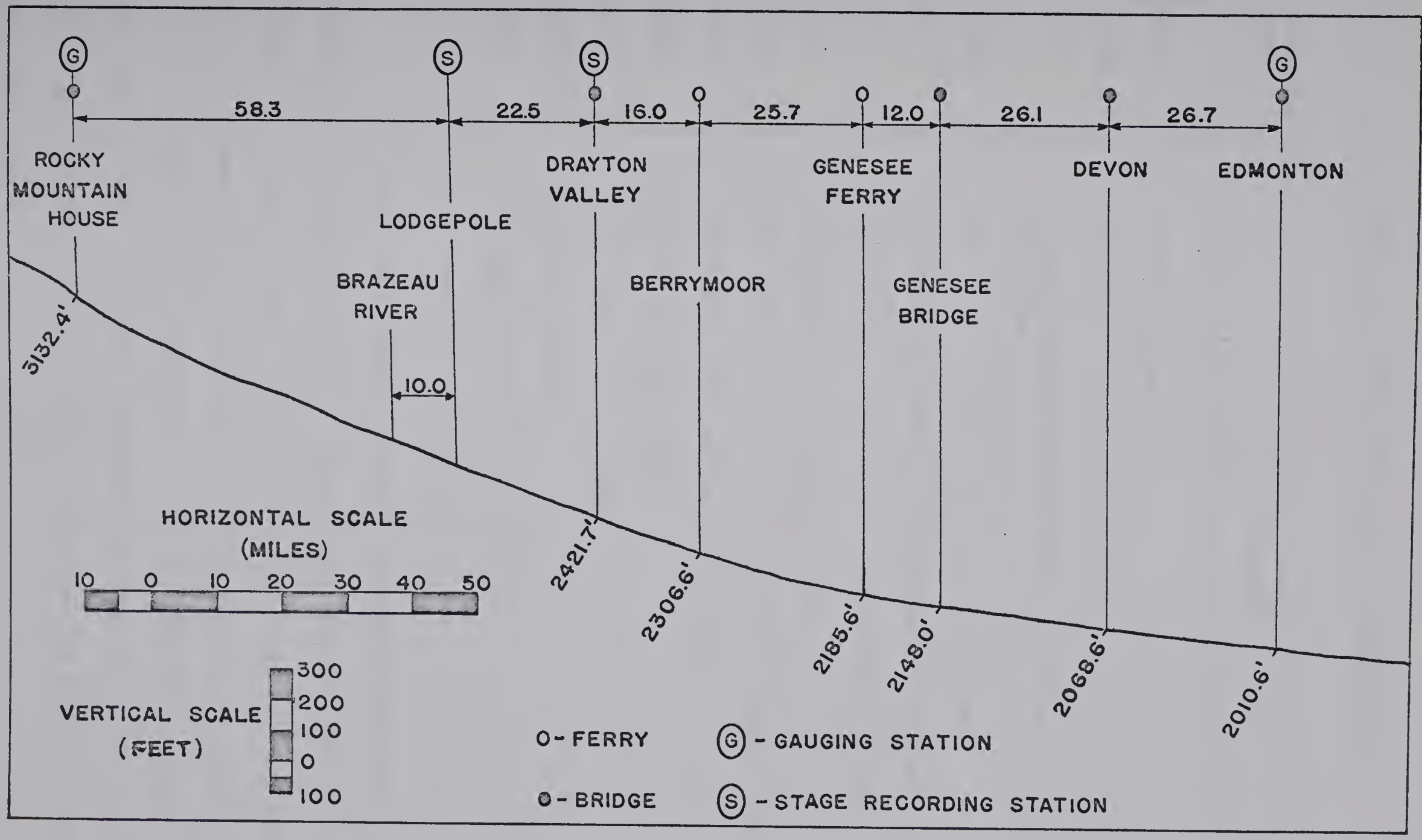


FIGURE 5-2 LONGITUDINAL PROFILE OF THE NORTH SASKATCHEWAN RIVER

TABLE 5.1 - NAME AND PURPOSE OF SUBROUTINES

| NAME | PURPOSE |
|---|---|
| WAV 21 | Control Program |
| SCRIB | Writes out T, X, W, Y from VECTR |
| SORT | Find maximum depth and maximum and minimum velocities for plot scales. |
| REACH | Calculates interior points on X-T diagram |
| BDY 1 | Left Boundary Condition (Discharge versus time) |
| BDY 2 | Right Boundary Condition (Stage-Discharge Curve) |
| TABL | Interpolating for values in tables |
| SHIFT | Shift index values (calculated points become initial points) |
| VECTR | Stores calculated values in one array |
| DNORM | Calculates normal depth |
| DCRIT | Calculates critical depth |
| WAVPLOT | Main plot program |
| SORTX | Arrangement of array for plotting |

As written, the program has several limitations which may require changing for different problems. The only end boundary conditions programmed are those of known flow rates and water levels. There are no provisions made for varying slope or cross-section of the channel, and it is also assumed that the roughness is constant throughout, regardless of the depth of flow. Since the prediction-corrector method is used to obtain the solution, accuracy tests are required and these may need changing, depending on the accuracy sought.

## 5.4 Testing the Program

As a check on the accuracy of the program, the computer solutions were compared to the field observations. Tests were initially run on open channel conditions and then the program was tested with an ice cover imposed on the channel. From the available field data the channel cross-section was assumed to be trapezoidal with a base of 210 feet and side slopes 1:15. The bed slope was considered to be the average slope over the portion of channel analyzed, while the Manning's n was taken as 0.029 for open channel flow and 0.023 for flow under the ice cover.

For the open channel flow tests, a section of the North Saskatchewan River from Lodgepole to Edmonton was used as the test section. The upstream boundary condition was stage versus time, while the downstream boundary condition was the rating curve. Surges of various heights and frequency were imposed at the upstream end of the channel and they were allowed to propagate downstream under various conditions. Plots of velocities and depths for all runs performed are shown in Chapter VI.

The tests for ice cover conditions were carried out with some variations, such as, the test section used was that of the North Saskatchewan River from the Brazeau River junction to Edmonton. The upstream boundary condition was discharge versus time, with the downstream boundary condition being the open water stage-discharge curve. The imposed discharge at the upstream end was the sum of the discharges at Rocky Mountain House and the Big Bend Plant. The fluctuations in flow only occur at the Big Bend Plant gauge, therefore it was necessary to estimate the time required for these variations to propagate the ten miles downstream to the junction of the North Saskatchewan River. The remainder of the testing procedure was similar to that of the open channel flow condition.

# CHAPTER VI

# RESULTS

## 6.1 General

The results of the computer simulation of wave propagation are best shown by means of plots. Plotting depth and velocity against distance and time fully describes the changes which occur in the surge as it progresses downstream.

## 6.2 Plots

The plots on the following pages are the results obtained from the runs performed. As the channel properties were varied for various runs, the conditions imposed on each run are listed with the resulting plots.

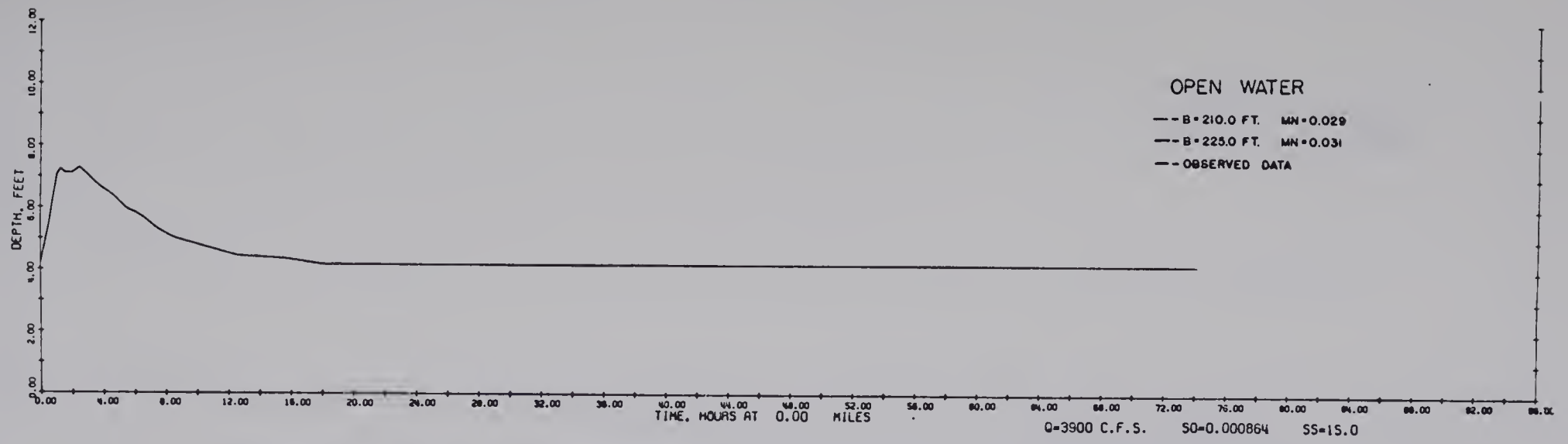


FIGURE 6-1 WATER LEVELS AT UPSTREAM END

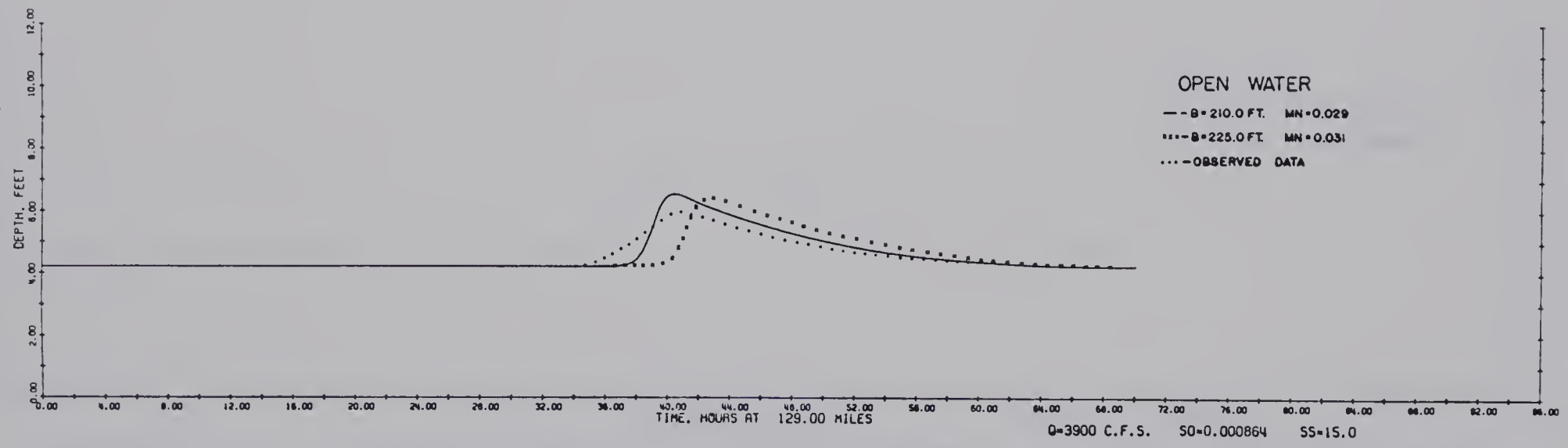


FIGURE 6-2 COMPARISON OF WATER LEVELS AT DOWNSTREAM END

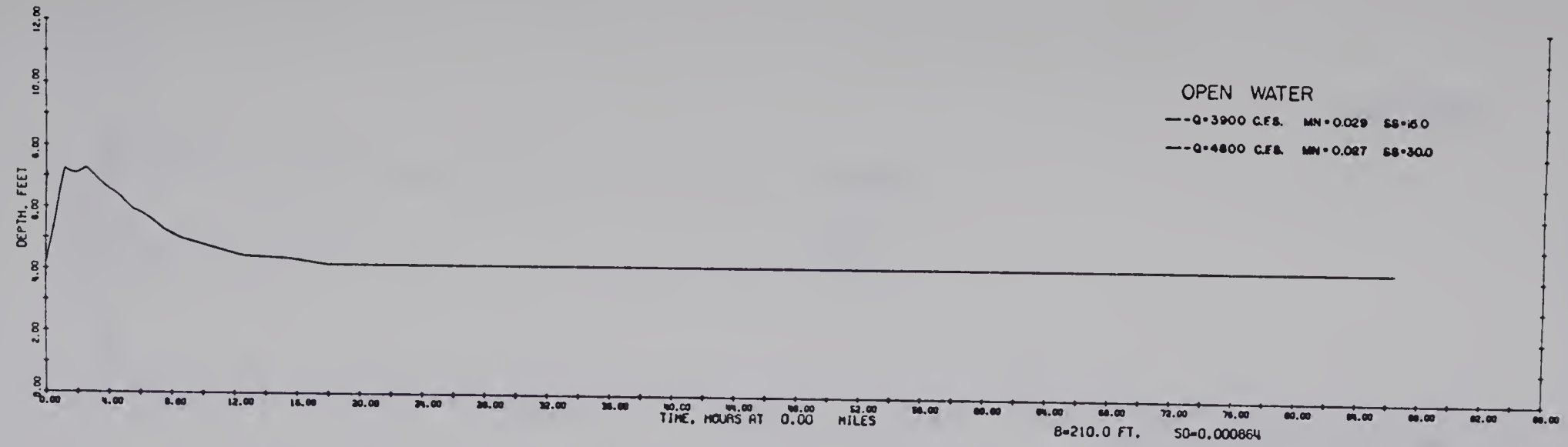


FIGURE 6-3 WATER LEVELS AT UPSTREAM END

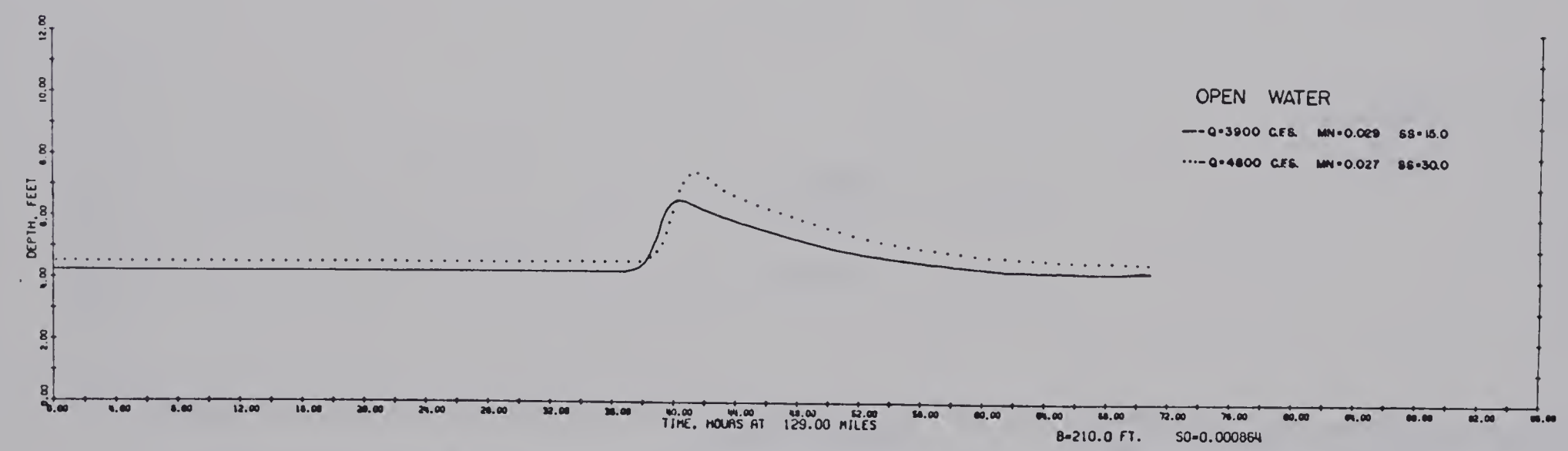


FIGURE 6-4 COMPARISON OF WATER LEVELS AT DOWNSTREAM END

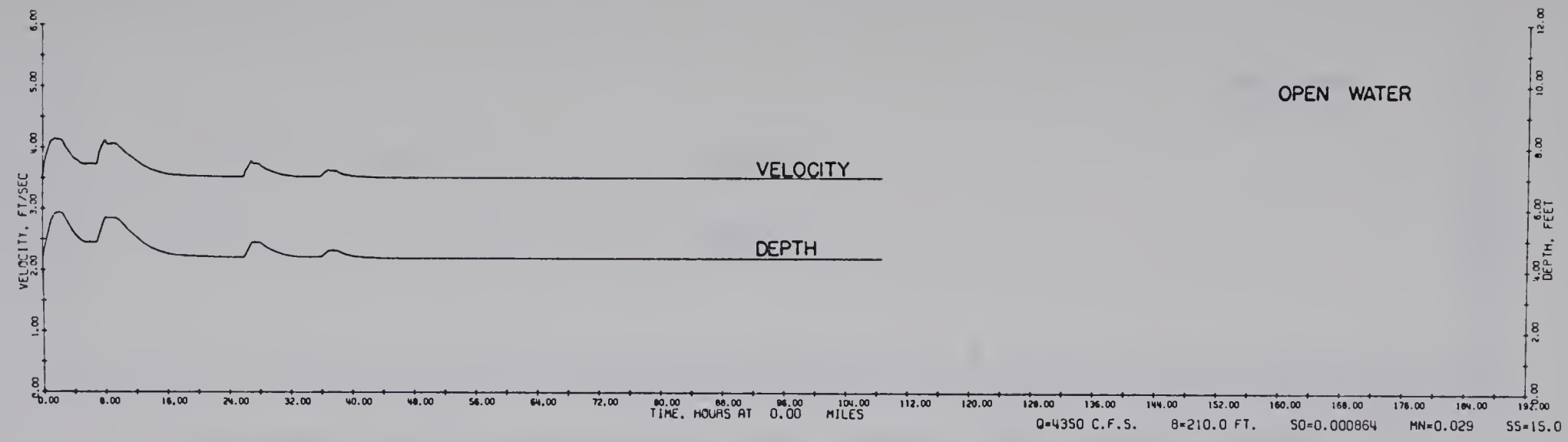


FIGURE 6-5 VELOCITY AND DEPTH AT UPSTREAM END

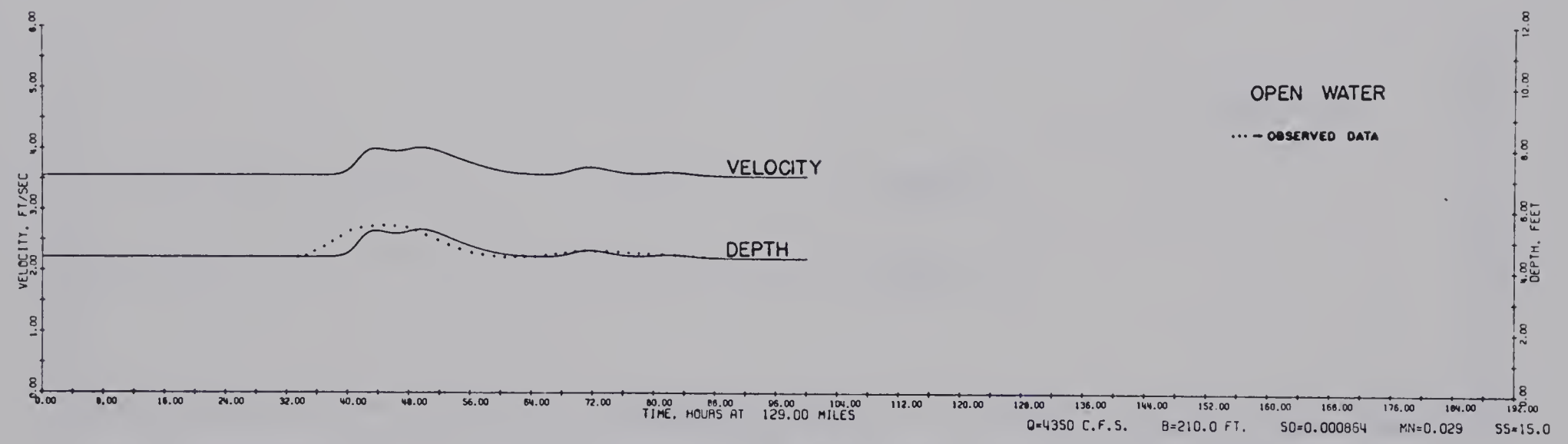


FIGURE 6-6 VELOCITY AND DEPTH AT DOWNSTREAM END

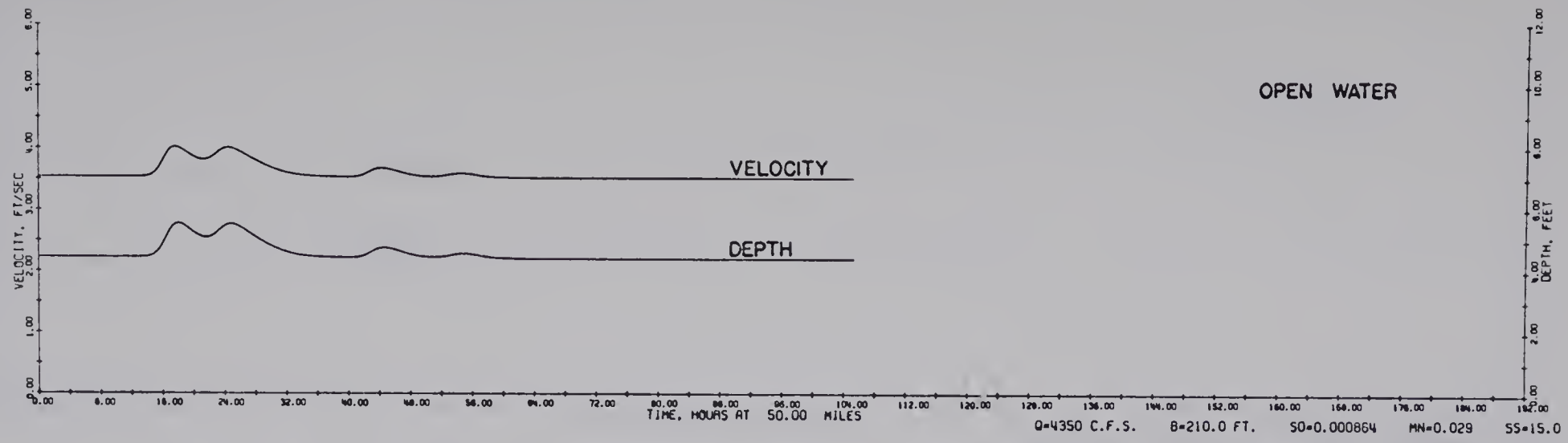


FIGURE 6-7 VELOCITY AND DEPTH AT 50.0 MILES

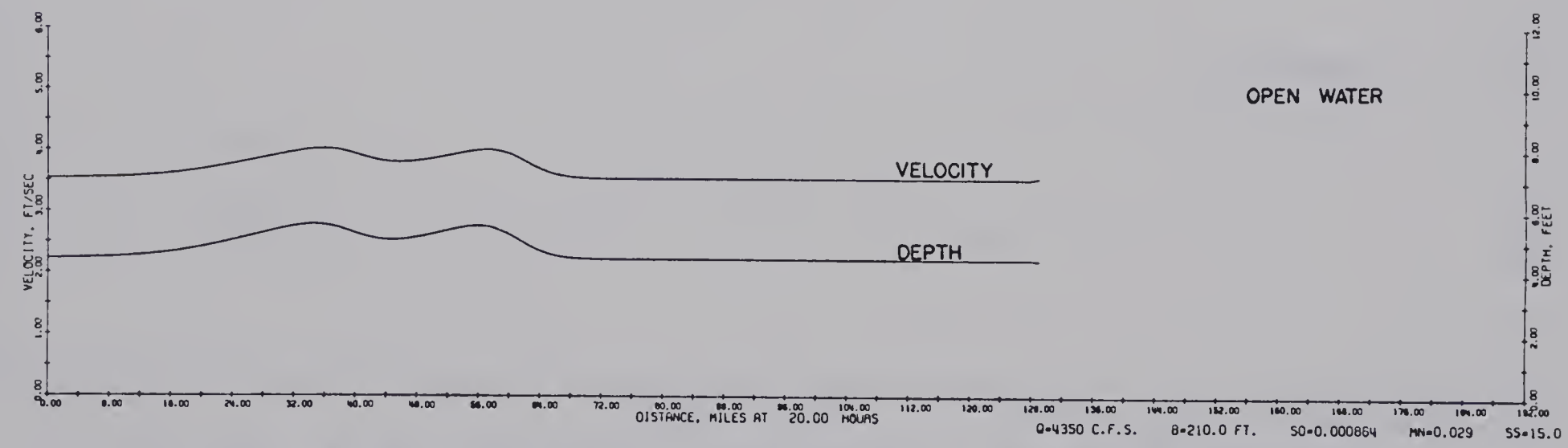


FIGURE 6-8 VELOCITY AND DEPTH AT 20.0 HOURS

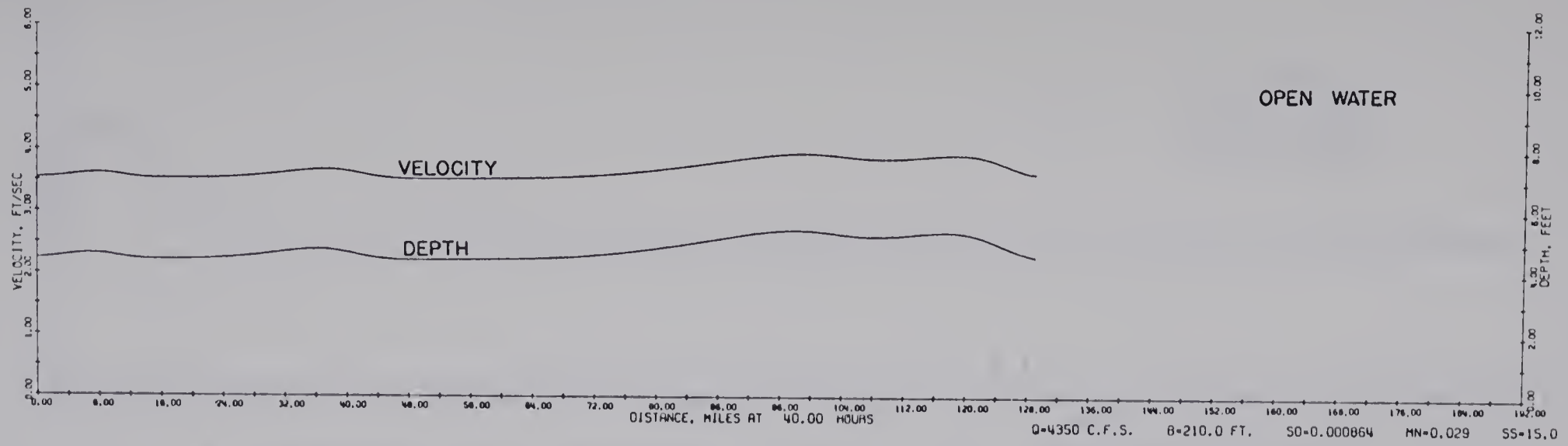


FIGURE 6-9 VELOCITY AND DEPTH AT 40.0 HOURS

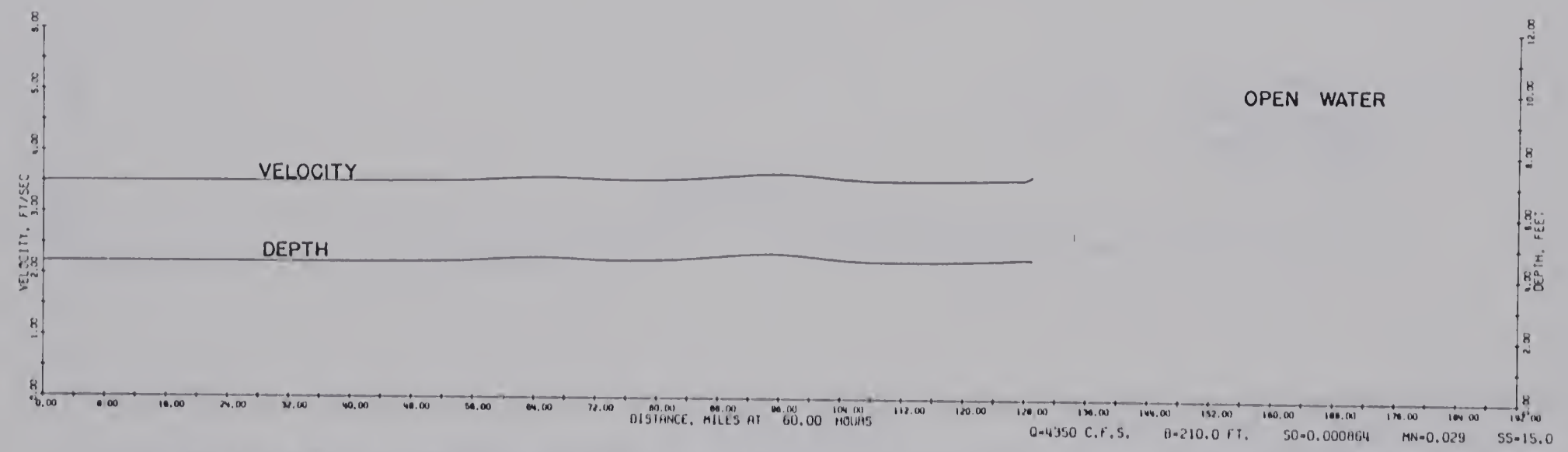


FIGURE 6-10 VELOCITY AND DEPTH AT 60.0 HOURS

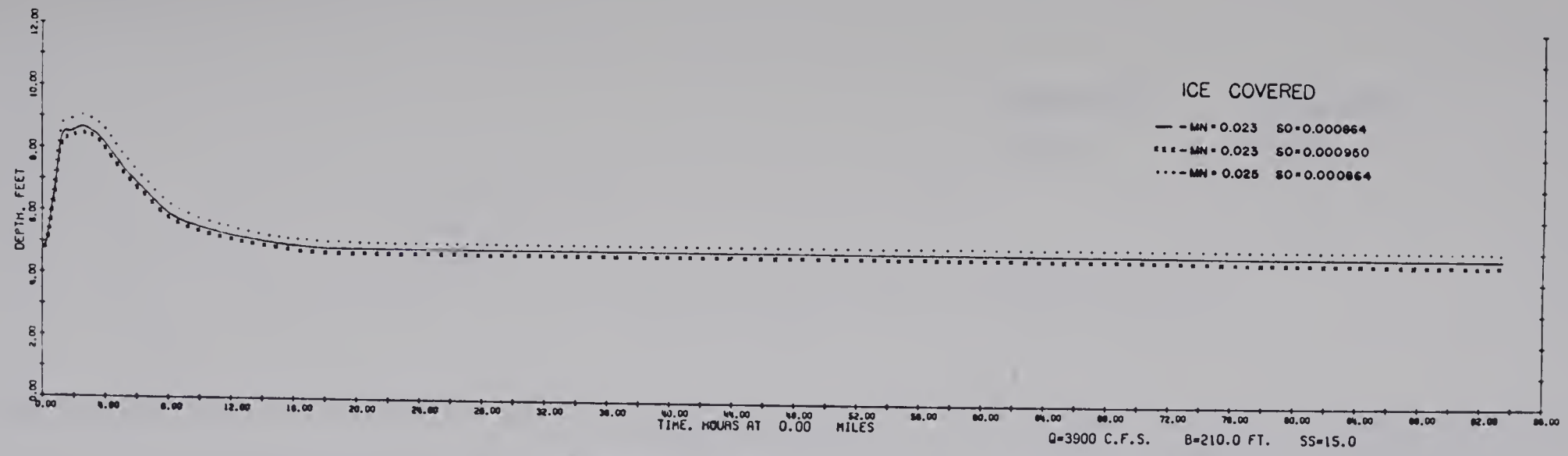


FIGURE 6-11 WATER LEVELS AT UPSTREAM END

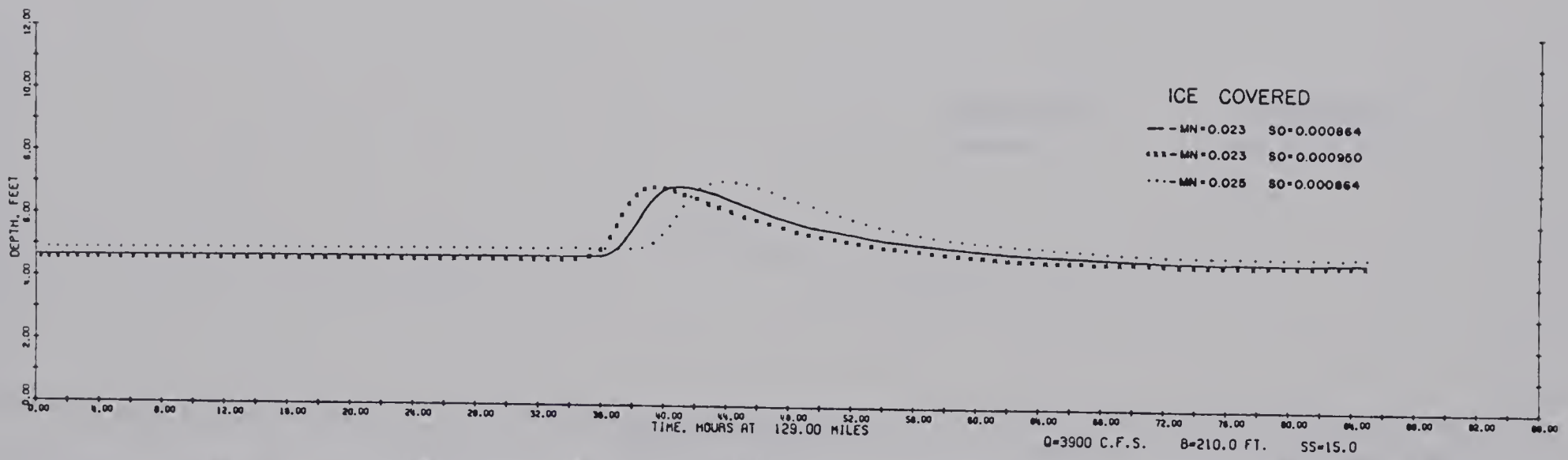


FIGURE 6-12 COMPARISON OF WATER LEVELS AT DOWNSTREAM END

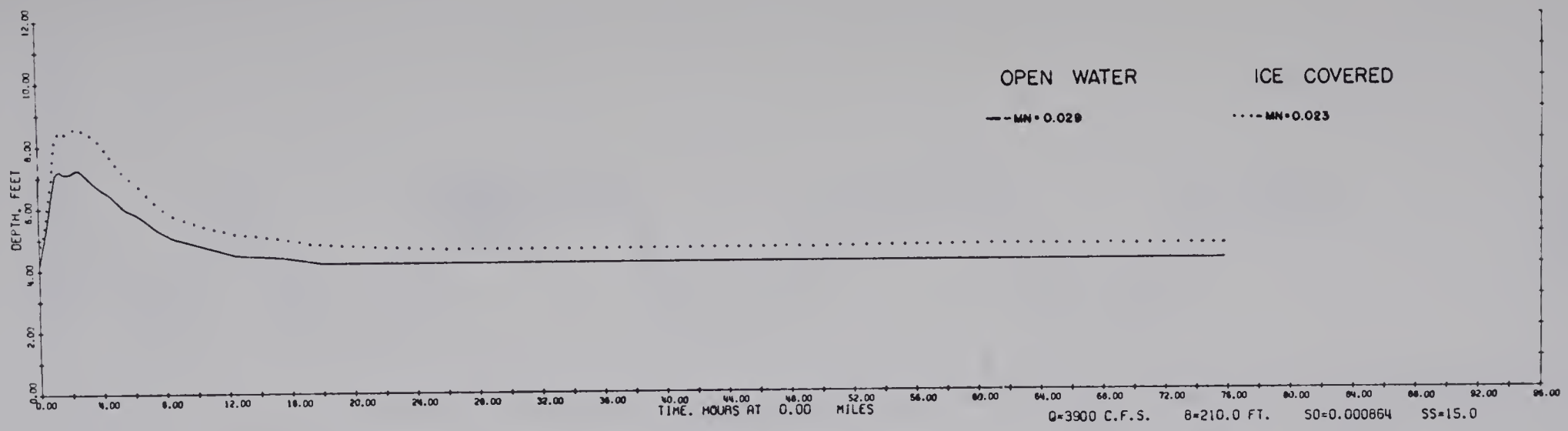


FIGURE 6-13 WATER LEVELS AT UPSTREAM END

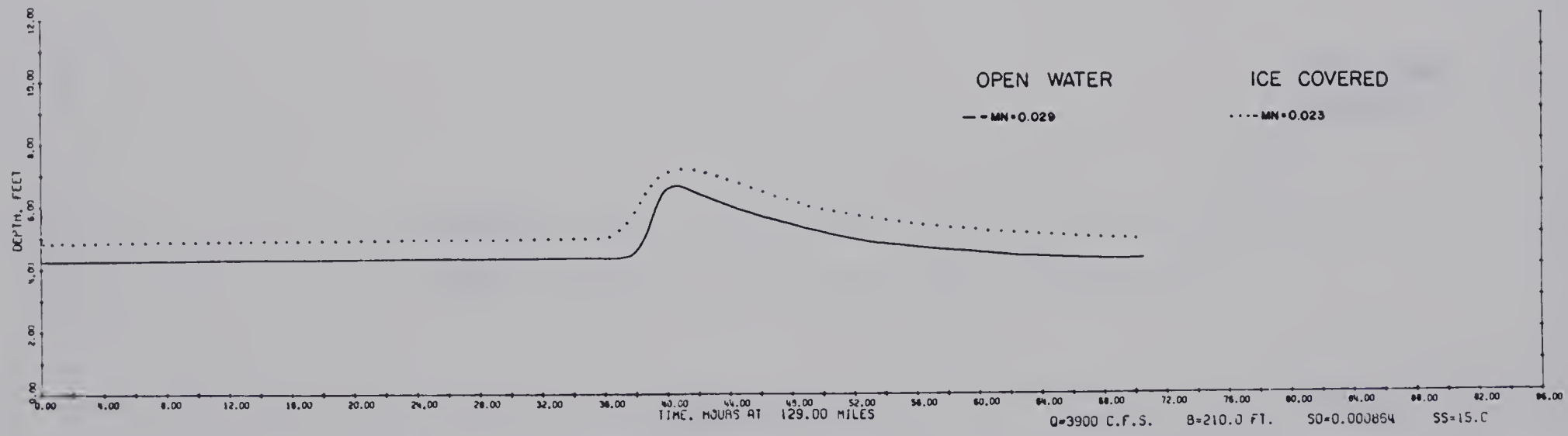


FIGURE 6-14 COMPARISON OF WATER LEVELS AT DOWNSTREAM END

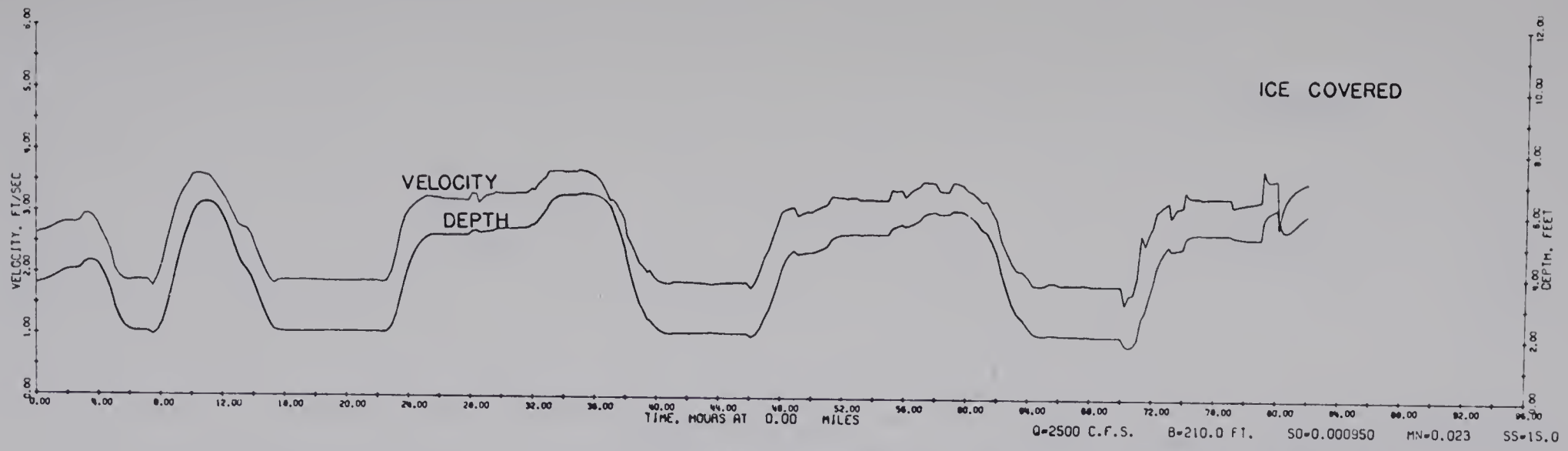


FIGURE 6-15 VELOCITY AND DEPTH AT UPSTREAM END

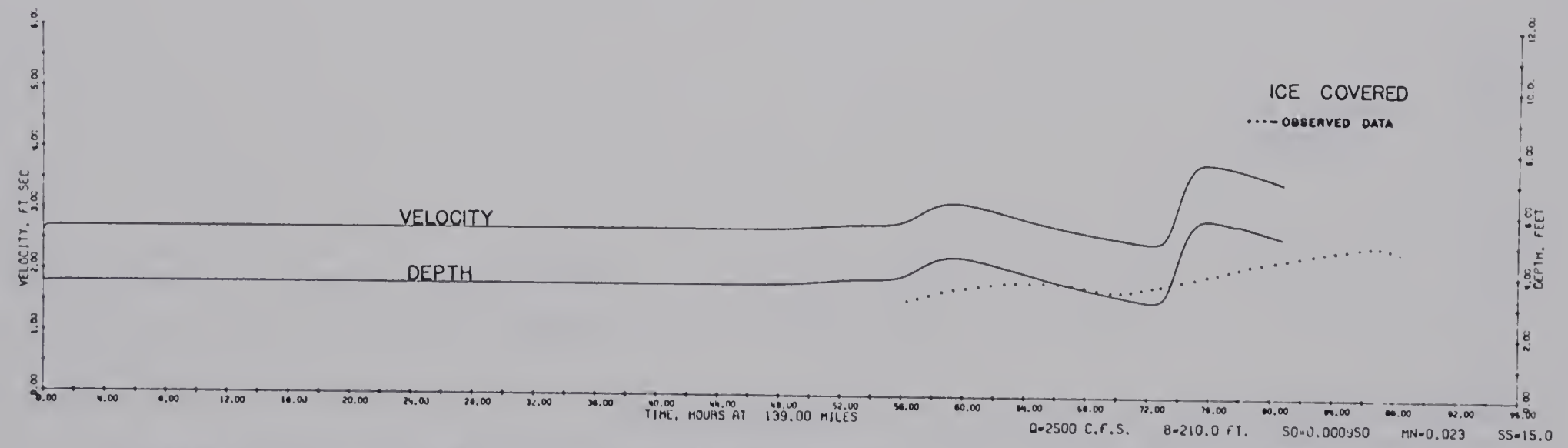


FIGURE 6-16 VELOCITY AND DEPTH AT DOWNSTREAM END

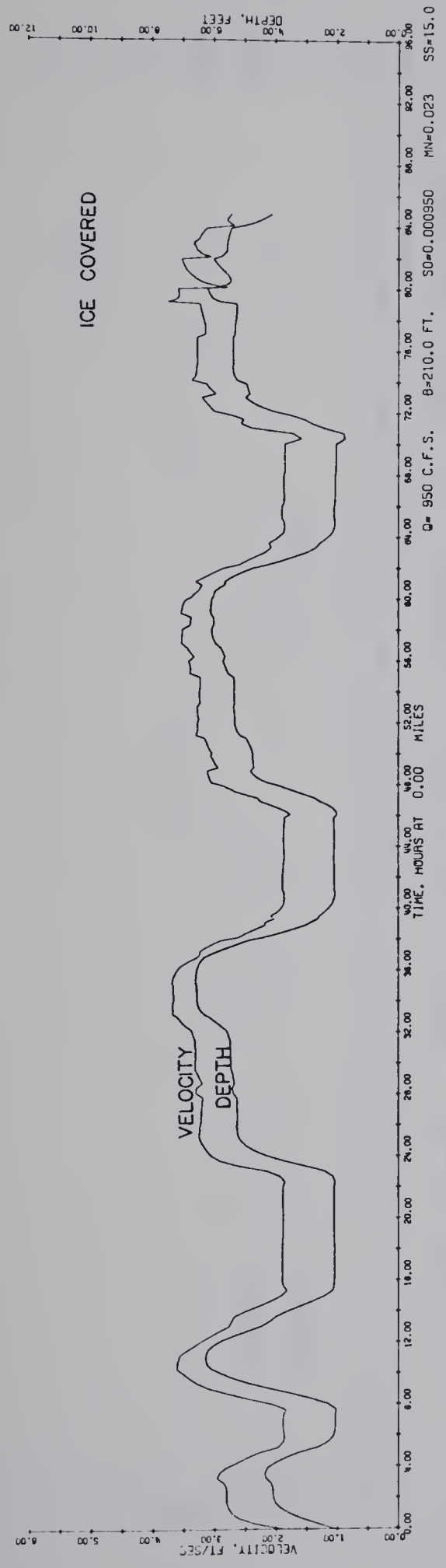


FIGURE 6-17 VELOCITY AND DEPTH AT UPSTREAM END

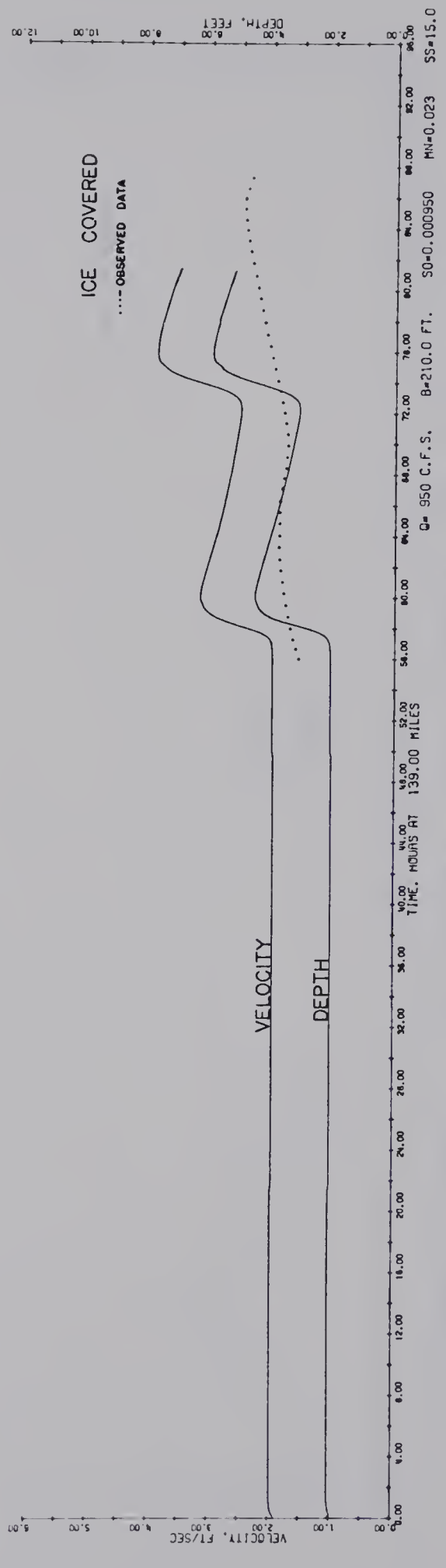


FIGURE 6-18 VELOCITY AND DEPTH AT DOWNSTREAM END

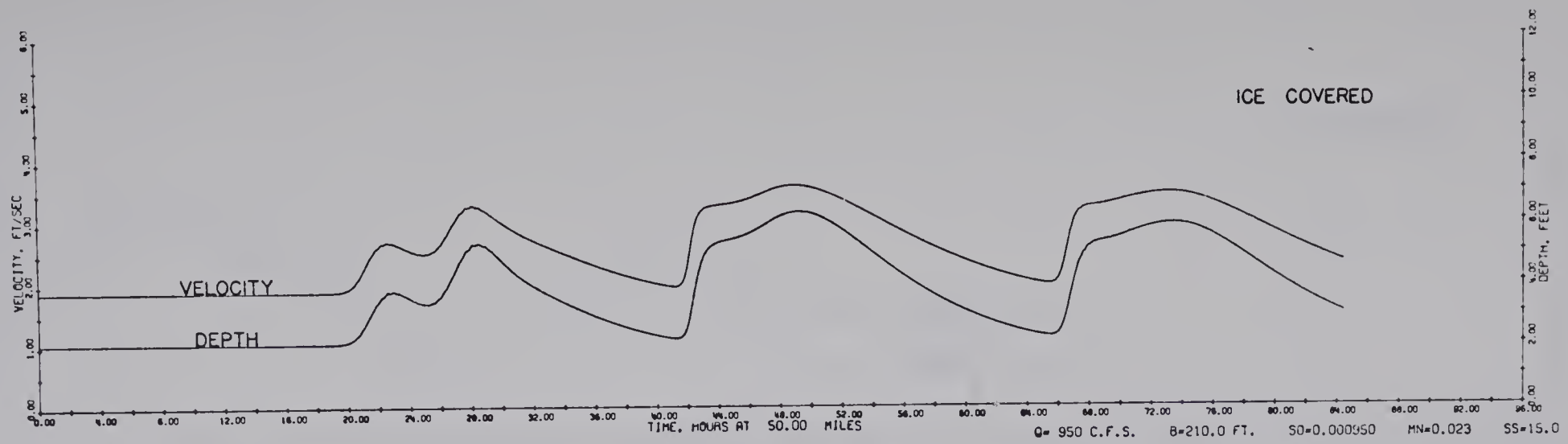


FIGURE 6-19 VELOCITY AND DEPTH AT 50.0 MILES

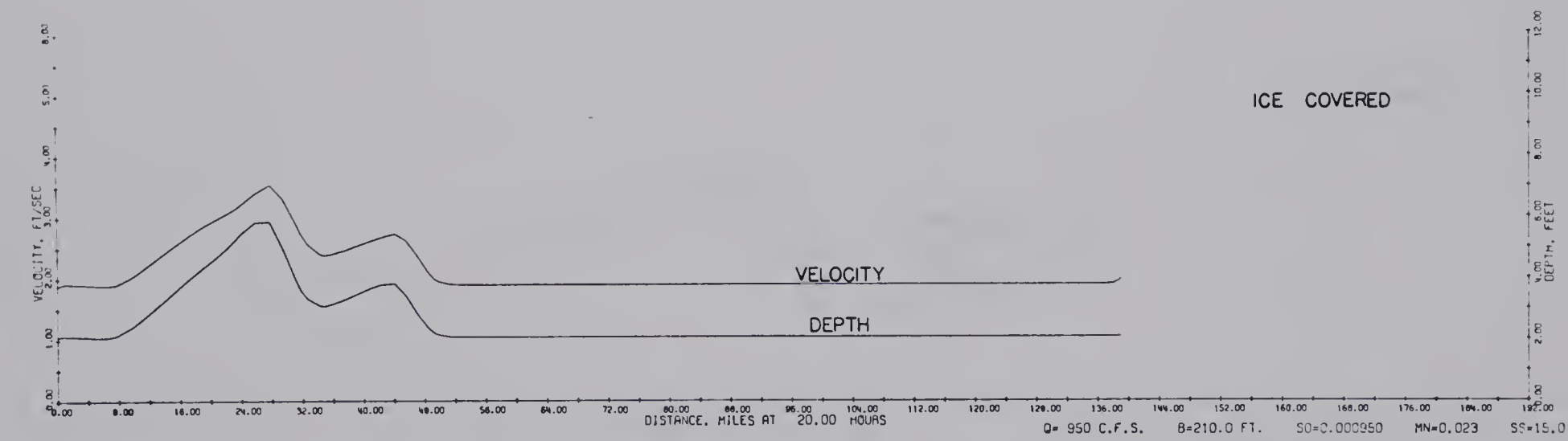


FIGURE 6-20 VELOCITY AND DEPTH AT 20.0 HOURS

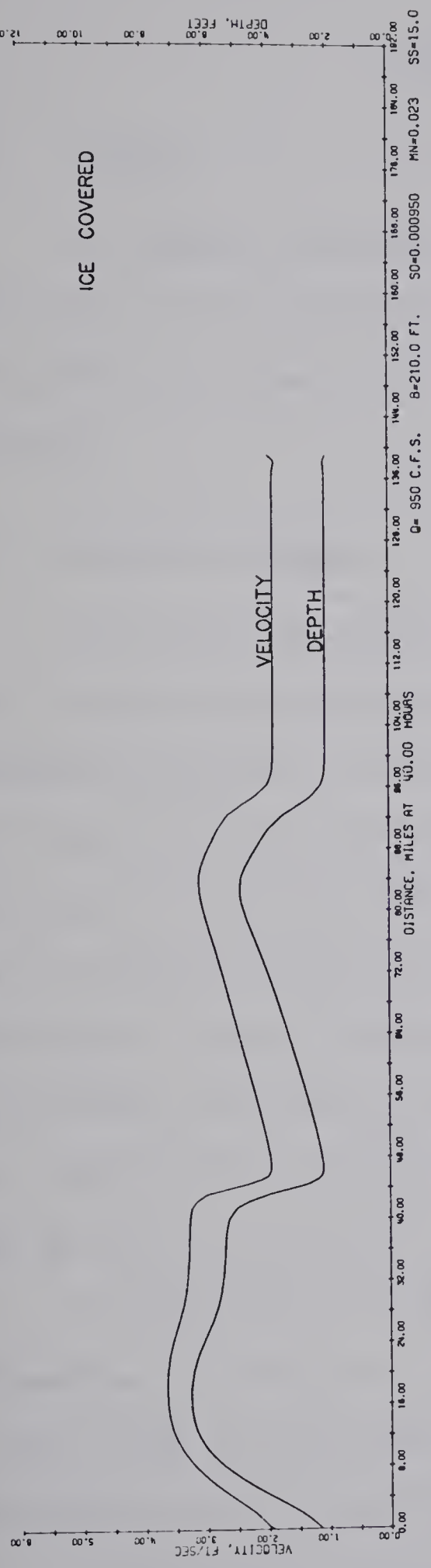


FIGURE 6-21 VELOCITY AND DEPTH AT 40.0 HOURS

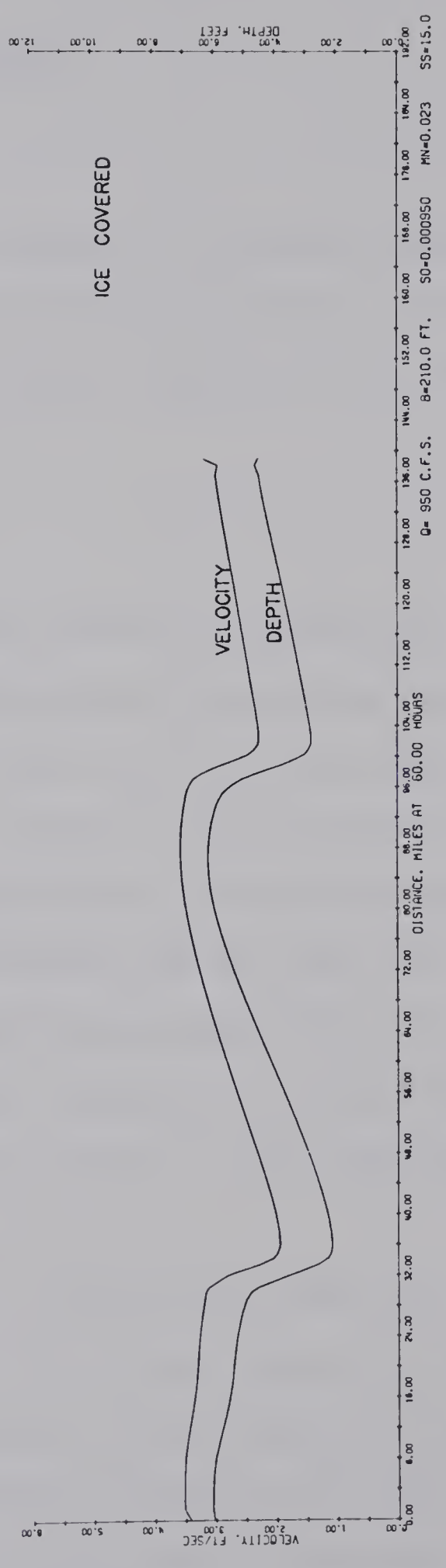


FIGURE 6-22 VELOCITY AND DEPTH AT 60.0 HOURS

# CHAPTER VII

# DISCUSSION OF RESULTS

## 7.1 General

This chapter discusses the results recorded in the previous chapter. The graphs provide an easy means of comparing the various results. The discussion mainly deals with the effect of channel roughness on the surge profiles.

## 7.2 Open-Water Surges

The results of open-water surges were plotted on Figures 6-1 to 6-10. Both the calculated and observed results for a single surge were plotted on Figure 6-2. The surge plotted with a solid line represents the calculated results for the conditions most closely related to natural conditions. The travel time calculated was similar to the observed value but the observed height of surge was approximately 25% less than that calculated. The only difference between the two calculated runs was a 7% increase in the value of n. A noticeable flattening of the surge occurs as a result of the increased roughness. The decrease in surge amplitude was 6% while the increase in travel time was 6%.

In Figures 6-3 and 6-4, an increase of 100% in side slopes and a 7% decrease in n resulted in an increase of 5% in travel time and an increase of 20% in surge height. The difference in initial depths at the downstream end was a result of the stage-discharge boundary condition.

The remaining figures of open-water surges depict a series of

surges propagating downstream in the channel. These figures show predicted profiles of the channel at various times as well as the predicted stage recordings for various stations. This gives a good description of the surge as it progresses downstream. The computed travel time was 8% less than the observed time. The amplitude of the observed surge was approximately 15% higher than that calculated for the largest surge. The smaller the amplitude the more closely related were the calculated and observed values for both travel time and surge height.

In general, the open-water surges behaved as expected. The variations between predicted and observed results increased with an increase in surge height. An increase in the roughness coefficient increased the travel time and decreased the height of the surge. This resulted in the surge becoming flatter and broader.

## 7.3 Surges Under Ice Cover

The remaining figures from Figure 6-11 to 6-22 inclusive are the results of surges propagating down a channel under an ice cover. In Figures 6-11 and 6-12 the same discharge was imposed at the upstream end but the conditions of the channel were varied for each run. Figure 6-13 and 6-14 compare surges in open water and under an ice cover. The remaining runs were concerned with a series of surges propagating down the channel.

An increase of 8% in the value of n produced an increase of 7% in travel time but the height of the surge was reduced by only a slight amount. The shapes of the surges were very similar in both cases. An increase of 10% in the channel slope resulted in a decrease of 5% in the

travel time of the surge and an increase of 6% in the height of the surge. Therefore, the surge had a sharper crest and was not spread out over as large a distance.

Figures 6-15 to 6-22 are the results of tests performed on a series of surges propagating down the channel. The only difference in the two runs was the initial discharge. The variation in initial condition of the channel only effected the profile of the first surge. The channel stabilized quickly, resulting in subsequent surges having the same profile regardless of the initial conditions imposed. The observed data plotted on the figures had different initial conditions than the calculated results, thus the only valid comparison would be to compare the second surge. The predicted travel time was 12% less than observed time and the predicted height of surge was 36% greater than observed height of surge.

From the tests performed, the ice cover did not appear to have as much effect as observed in the field. There was a large variation in the calculated and observed conditions for the runs under ice cover. Although the calculated results showed that the surge was damped considerably due to the ice cover, it was not as large as the actual damping. Possibly the calculated roughness coefficient was not as large as the actual value.

## 7.4 Comparison of Open Water Surges and Surges Under an Ice Cover

The results of a single surge propagating down a channel under various conditions are tabulated in Table 7.1. No. 2 and 4 are the natural conditions for the North Saskatchewan River and are compared in Figures 6-13 and 6-14. For open water the decrease in surge height over the reach was 20% and under an ice cover it was 45%. The ice caused a considerable damping of the surge. The travel time of the surge for

TABLE 7.1 - SUMMARY OF COMPUTED SURGE DATA

| No. | Channel Cover | n | $S_{X10^{-3}}$ | SS | Upstream Surge Height (ft) | Downstream Surge Height (ft) | Travel Time (hrs) |
|---|---|---|---|---|---|---|---|
| 1 | Open | 0.027 | 8.64 | 30.0 | 3.0 | 2.8 | 42 |
| 2 | Open | 0.029 | 8.64 | 15.0 | 3.0 | 2.4 | 41 |
| 3 | Open | 0.031 | 8.64 | 15.0 | 3.0 | 2.2 | 43 |
| 4 | Ice | 0.023 | 8.64 | 15.0 | 3.9 | 2.3 | 41 |
| 5 | Ice | 0.025 | 8.64 | 15.0 | 4.0 | 2.2 | 44 |
| 6 | Ice | 0.023 | 9.50 | 15.0 | 3.9 | 2.3 | 39 |

the two conditions was similar even though the initial velocity was less for the ice cover condition. This occurs because the surge has a greater height under ice cover thus the celerity of the surge increases.

Even though the calculated results showed some large fluctuations from observed values, the results did show that an ice cover causes considerable change to the profile of the surge.

## 7.5 Computer Techniques

The computer provided a very necessary tool in performing the calculations for the numerical analysis of this study. Discrepancies in the results produced by these techniques are small compared to those produced by the broad assumptions used in the analysis. In Figures 6-15 and 6-17, the discharge data was very irregular but small errors become noticeable after a time of 70 hours. The effect produced by these errors was negligible.

# CHAPTER VIII

# CONCLUSIONS AND RECOMMENDATIONS

## 8.1 General

A review of the literature indicated a lack of information on surges as well as the roughness coefficients in ice covered channels. The present study was initially concerned with the evaluation of composite roughness coefficients and then applying these results to surges propagating down ice covered channels.

## 8.2 Conclusions

The addition of an ice cover results in considerable change in the channel roughness. Even though the numerical coefficient of roughness for an ice covered channel is less than that for an open channel, the effect of the roughness is increased as a result of the increase in wetted perimeter. During the mid-winter period on the North Saskatchewan River, Manning's n for the ice cover can be approximated as 0.015. This is approximately 1/2 the value of n for open channel conditions at low flows. Thus an approximate value for a composite roughness coefficient to be applied to the entire channel during ice cover would be 0.023. On the basis of the roughness coefficient of the ice cover being 1/2 the roughness of the bed, the depth of flow would increase 12% due to the ice cover. Stage readings would increase an additional amount equal to the bouyant thickness of the ice cover. During the period of freeze-up and break-up, the roughness coefficient is increased to a much greater extent but it is very difficult to estimate this increase as it varies from year to year depending on the climatic conditions.

From the results obtained, the ice cover had a significant effect on the characteristics of a surge. The ice cover had little effect on the travel time of the surge even though the flow velocity decreases. This is a result of the increase in celerity of the surge due to its increase in height. The ice cover also causes a greater damping of the surge.

The method of characteristics combined with the numerical techniques applied did not produce as accurate results as would be desirable. Much of the variations in results can be contributed to the limited amount of channel geometry applied and the large length of channel considered. As an estimate of surge properties for design purposes, this method could be considered since it gives surges at the downstream end which are higher than observed surges.

## 8.3 Recommendations

In view of the present study there is a great need for more study in this area in order that the effect of an ice cover on surges may be better understood. It is therefore recommended that:

(a) there is further study on the composite roughness coefficient produced by an ice cover with particular attention on the freeze-up and break-up period.

(b) test be conducted to determine the effect of various changes in channel geometry and boundary conditions used with a computer program in an attempt to verify or limit the conclusions of this study.

## LIST OF REFERENCES

Baltzer, R. A. and Chintu Lai, Computer Simulation of Unsteady Flows in Waterways. A.S.C.E., vol. 94, No. HY4, pp. 1083-1117, July, 1968.

Bennett, R. M., The Stage-Discharge Relationship and Winter Discharge Under Ice Cover for the Peace and Slave Rivers. M.Sc. Thesis, Utah State University, Logan, Utah, 1968.

Campbell, R. I., Report on Activities in Calgary District During Winter of 1965-66. Internal Report, Water Survey of Canada, Calgary, 1966.

Carey, K. L., Analytical Approaches to Computation of Discharge of an Ice-Covered Stream. U.S. Geol. Survey Prof. paper, 575-C. pp. 0200-0207, 1967.

Chow, Ven Te, Handbook of Applied Hydrology. McGraw-Hill Book Company, pp. 10-46, 16-7, 1964.

Collins, J. I. and Fersht, S. N., Mixed Technique for Computing Surges in Channels. A.S.C.E., vol. 94, No. HY2, pp. 349-362, March, 1966.

Cooper, R. H., The Effect of a Surface Cover on Open Channel Surges. M.Sc., Thesis, University of Alberta, Edmonton, Alberta, 1966.

Grushevskiy, M. S., Some Problems of Unsteady Movements in Natural Channels and Bodies of Water. Soviet Hydrology, selected papers, American Geophysical Union, pp. 1-12, 1965.

Hoyt, G. W., The Effects of Ice on Stream Flow. U.S. Geol. Survey Water Supply. Paper 337, 1913.

Kamphuis, J. W., Mathematical Tidal Study of St. Lawrence River. A.S.C.E., vol. 96, No. HY3, pp. 643-664, March, 1970.

Keulegan, G. H., Laws of Turbulent Flow in Open Channels. Journal of Research of the National Bureau of Standards, U.S. Dept. of Commerce, vol. 21, paper RP1151, Dec., 1938.

Kolupaila, Prof. S., The River Flow Beneath the Ice. Transactions of International Commissions of Snow and Glaciers, International Association of Scientific Hydrology. Bulletin No. 23, pp. 297-308, 1936.

Larsen, P. A., Head Losses Caused by an Ice Cover on Open Channels. Boston Society of Civil Engineers, Journal. Vol. 56, No. 1, pp. 45-67, January, 1969.

Martin, C. S. and De Fazio, F. G., Open-Channel Surge Simulation by Digital Computer. A.S.C.E., vol. 95, No. HY6, pp. 2049-2070, November, 1969.

Morton, G. H., Report on the Activities in Calgary District During Winter of 1966-67. Internal Report, Water Survey of Canada, Calgary, 1967.

Nezhikhovskiy, R. A., Coefficients of Roughness of Bottom Surface of Slush Ice Cover. Soviety Hydrology, selected papers, American Geophysical Union, No. 2, pp. 127-150, 1964.

Tillinghast, F. H., Records of Flow at Current-Meter Gauging Stations When the Streams are Subject to Ice. Eng. News, vol. 53, pp. 491-492, 1905.

# APPENDIX A

## DATA COLLECTED

TABLE A.1

STAGE-DISCHARGE READINGS AT EDMONTON

| DATE | STAGE* | DISCHARGE** |
|---|---|---|
| OCT/69 | | |
| 1 | 2064.1 | 5190 |
| 2 | 2063.8 | 4360 |
| 3 | 2063.7 | 4080 |
| 4 | 2063.7 | 4160 |
| 5 | 2063.7 | 4270 |
| 6 | 2063.7 | 4270 |
| 7 | 2063.5 | 4010 |
| 8 | 2063.4 | 3800 |
| 9 | 2063.4 | 3740 |
| 10 | 2064.2 | 5440 |
| 11 | 2063.6 | 4080 |
| 12 | 2063.6 | 4020 |
| 13 | 2063.6 | 4080 |
| 14 | 2063.6 P | 4060 |
| 15 | 2063.4 P | 3850 |
| 16 | 2063.4 | 3580 |
| 17 | 2063.4 | 3480 |
| 18 | 2063.3 | 3340 |
| 19 | 2063.1 | 3180 |
| 20 | 2063.0 | 3010 |
| 21 | 2063.0 | 2980 |
| 22 | 2063.3 | 3450 |
| 23 | 2063.1 | 3110 |
| 24 | 2063.2 | 3240 |
| 25 | 2063.1 | 3120 |
| 26 | 2063.1 | 3050 |
| 27 | 2063.0 | 2780 |
| 28 | 2062.9 | 2610 |
| 29 | 2062.9 | 2450 |
| 30 | 2062.8 | 2360 |
| 31 | 2062.9 | 2360 |
| NOV/69 | | |
| 1 | 2063.0 | 2740 |
| 2 | 2063.0 | 2710 |
| 3 | 2063.1 | 2630 |
| 4 | 2063.1 | 2610 |
| 5 | 2063.1 | 2670 |
| 6 | 2063.1 | 2740 |
| 7 | 2063.1 P | 2760 |
| 8 | 2063.1 | 2570 |
| 9 | 2062.9 | 2340 |
| 10 | 2063.0 | 2480 |
| 11 | 2063.0 | 2340 |
| 12 | 2063.3 | 2980 |
| 13 | 2063.3 | 2700 |
| 14 | 2063.4 | 2910 |
| 15 | 2064.0 | 4800 |
| 16 | 2063.9 | 4040 |
| 17 | 2064.6 | 3690 |
| 18 | 2064.5 | 1770 |
| 19 | 2067.2 | 5700 |
| 20 | 2066.9 | 4040 |
| 21 | 2067.0 | 2180 |
| 22 | 2067.5 | 3010 |
| 23 | 2067.4 | 3000 |
| 24 | 2067.3 P | 3300 |
| 25 | 2067.3 P | 3610 |

TABLE A.1 CONTINUED

| DATE | STAGE* | DISCHARGE** |
|---|---|---|
| 26 | 2067.2 P | 3150 |
| 27 | 2067.2 | 3100 E |
| 28 | 2067.3 P | 3100 E |
| 29 | 2067.1 | 3100 E |
| 30 | 2066.6 | 3100 E |
| DEC/69 | | |
| 1 | 2066.4 | 2670 |
| 2 | 2066.1 P | 2960 |
| 3 | 2066.0 | 2890 |
| 4 | 2065.7 P | 2530 |
| 5 | 2065.8 | 2700 |
| 6 | 2065.6 | 2570 |
| 7 | 2065.4 | 2470 |
| 8 | 2065.4 | 2570 |
| 9 | 2065.1 | 2340 |
| 10 | 2064.7 | 2110 |
| 11 | 2064.7 | 1980 |
| 12 | 2064.6 | 1980 |
| 13 | 2064.5 | 1990 |
| 14 | 2064.7 | 2140 |
| 15 | 2064.9 | 2470 |
| 16 | 2065.3 | 2930 |
| 17 | 2065.1 | 2720 |
| 18 | 2064.8 | 2510 |
| 19 | 2064.1 | 2330 |
| 20 | 2064.8 | 2470 |
| 21 | 2064.7 | 2520 |
| 22 | 2064.5 | 2330 |
| 23 | 2064.4 | 2320 |
| 24 | 2064.4 | 2230 |
| 25 | 2064.4 | 2260 |
| 26 | 2064.6 | 2400 |
| 27 | 2064.7 | 2620 |
| 28 | 2064.5 | 2460 |
| 29 | 2064.5 | 2440 |
| 30 | 2064.4 | 2760 |
| 31 | 2064.4 | 2760 E |
| JAN/70 | | |
| 1 | 2064.3 | 2480 |
| 2 | 2064.6 | 2160 |
| 3 | 2064.6 | 2410 |
| 4 | 2064.7 | 2500 |
| 5 | 2065.0 | 2790 |
| 6 | 2065.0 | 3100 |
| 7 | 2064.9 | 2810 |
| 8 | 2064.6 | 2520 |
| 9 | 2064.4 | 2270 |
| 10 | 2064.5 | 2350 |
| 11 | 2064.4 | 2290 |
| 12 | 2064.2 | 2100 |
| 13 | 2064.2 | 2050 |
| 14 | 2064.4 | 2180 |
| 15 | 2064.5 | 2240 |
| 16 | 2064.6 | 2510 |
| 17 | 2064.6 | 2620 |
| 18 | 2064.5 | 2270 |
| 19 | 2064.4 | 2220 |
| 20 | 2064.3 | 2120 |

TABLE A.1 CONTINUED

| DATE | STAGE* | DISCHARGE** |
|---|---|---|
| 21 | 2064.4 | 2230 |
| 22 | 2064.5 | 2400 |
| 23 | 2064.5 | 2390 |
| 24 | 2064.6 | 2420 |
| 25 | 2064.5 | 2390 |
| 26 | 2064.4 | 2380 |
| 27 | 2064.3 | 2220 |
| 28 | 2064.3 | 2260 |
| 29 | 2064.3 | 2210 |
| 30 | 2064.3 | 2210 E |
| 31 | 2064.3 | 2210 E |
| FEB/70 | | |
| 1 | 2064.6 | 2450 |
| 2 | 2064.7 | 2460 |
| 3 | 2064.6 | 2420 |
| 4 | 2064.5 | 2320 |
| 5 | 2064.8 | 2580 |
| 6 | 2064.7 | 2480 |
| 7 | 2064.6 | 2420 |
| 8 | 2064.6 | 2390 |
| 9 | 2064.4 | 2260 |
| 10 | 2064.6 | 2390 |
| 11 | 2064.7 | 2420 |
| 12 | 2064.7 | 2510 |
| 13 | 2064.7 | 2590 |
| 14 | 2064.8 | 2620 |
| 15 | 2064.9 | 2790 |
| 16 | 2064.9 | 2930 |
| 17 | 2064.7 | 2630 |
| 18 | 2064.7 | 2560 |
| 19 | 2064.9 | 2830 |
| 20 | 2064.9 | 2810 |
| 21 | 2064.9 | 2790 |
| 22 | 2065.0 | 2970 |
| 23 | 2064.9 | 2910 |
| 24 | 2064.7 | 2750 |
| 25 | 2064.7 | 2610 |
| 26 | 2065.0 | 2710 |
| 27 | 2064.9 | 2700 E |
| 28 | 2064.9 | 2700 E |
| MARCH/70 | | |
| 1 | 2064.9 | 2850 |
| 2 | 2064.9 | 2930 |
| 3 | 2064.8 | 2680 |
| 4 | 2064.7 | 2570 |
| 5 | 2065.1 | 2740 |
| 6 | 2065.0 | 2590 |
| 7 | 2065.1 | 2710 |
| 8 | 2065.5 | 3340 |
| 9 | 2065.2 | 2960 |
| 10 | 2064.9 | 2570 |
| 11 | 2065.0 | 2520 |
| 12 | 2065.1 | 2760 |
| 13 | 2065.1 | 2830 |
| 14 | 2065.2 | 2840 |
| 15 | 2065.2 | 2830 |
| 16 | 2065.2 | 2790 |
| 17 | 2065.1 | 2800 |

TABLE A.1 CONTINUED

| DATE | STAGE* | DISCHARGE** |
|---|---|---|
| 18 | 2065.1 | 2540 |
| 19 | 2065.2 | 2920 |
| 20 | 2065.1 | 2680 |
| 21 | 2065.0 | 2440 |
| 22 | 2064.9 | 2320 |
| 23 | 2064.8 | 2210 |
| 24 | 2064.8 | 2220 |
| 25 | 2064.9 | 2330 |
| 26 | 2064.9 | 2270 |
| 27 | 2064.9 | 2290 |
| 28 | 2065.0 | 2450 |
| 29 | 2064.9 | 2360 |
| 30 | 2064.9 | 2200 |
| 31 | 2064.9 | 2210 |
| APRIL/70 | | |
| 1 | 2065.0 | 2470 |
| 2 | 2065.1 | 2460 |
| 3 | 2065.5 | 3040 |
| 4 | 2065.8 | 3950 |
| 5 | 2066.1 | 4500 |
| 6 | 2066.9 | 5630 |
| 7 | 2067.8 | 8210 |
| 8 | 2067.8 | 9890 |
| 9 | 2067.7 | 8700 |
| 10 | 2067.7 | 9030 |
| 11 | 2067.6 | 9130 |
| 12 | 2067.2 | 7800 |
| 13 | 2065.6 | 6760 |
| 14 | 2064.7 | 6200 |
| 15 | 2064.5 | 6000 |
| 16 | 2064.3 | 5150 |
| 17 | 2064.2 | 4860 |
| 18 | 2064.1 | 4720 |
| 19 | 2064.1 | 4720 |
| 20 | 2063.9 | 4560 |
| 21 | 2064.0 | 4800 |
| 22 | 2064.3 | 5100 |
| 23 | 2064.4 | 5460 |
| 24 | 2064.3 | 5230 |
| 25 | 2064.1 | 4740 |
| 26 | 2064.1 | 4700 |
| 27 | 2064.1 | 4760 |
| 28 | 2064.0 | 4380 |
| 29 | 2064.2 | 6260 |
| 30 | 2064.0 | 6000 E |

* STAGE AT MAYFAIR PARK GAUGE (CITY ELEVATION)

** DISCHARGE AT LOW LEVEL BRIDGE (CFS)

P PUMPING

E ESTIMATED

TABLE A.2

CURRENT-METERING

ON THE NORTH SASKATCHEWAN RIVER AT MAYFAIR PARK GAUGE

ON FEBRUARY 7, 1970

| SECTION | DEPTH | VELOCITY (fps) |
|---|---|---|
| #1 | FROZEN TO | |
| D = 100' | BOTTOM | |
| #2 | | |
| D = 125' | | |
| T.D. = 3'3" | | NO |
| I.T. = 1.85' | | VELOCITY |
| W.I. = -1.5" | | |
| #3 | | |
| D = 150' | | |
| T.D. = 4'3" | | NO |
| I.T. = 1.5' | | VELOCITY |
| W.I. = +0.5" | | |
| #4 | 4'3" | 0.85 |
| D = 162' | 3'9" | 1.19 |
| T.D. = 4'6" | 3'3" | 1.23 |
| I.T. = 1.5' | 2'9" | 1.45 |
| W.I. = +0.5" | 2'3" | 1.39 |
| | 2'0" | 1.32 |
| | 1'7" | 1.13 |

| SECTION | DEPTH | VELOCITY (fps) |
|---|---|---|
| #5 | 4'3" | 1.07 |
| D = 175' | 4'0" | 1.37 |
| T.D. = 4'6" | 3'9" | 1.47 |
| I.T. = 1.3' | 3'6" | 1.56 |
| W.I. = +0.5" | 3'3" | 1.68 |
| | 3'0" | 1.73 |
| | 2'9" | 1.73 |
| | 2'6" | 1.82 |
| | 2'3" | 1.82 |
| | 2'0" | 1.49 |
| | | 1.77 |
| | 1'9" | 1.59 |
| | 1'5" | 1.29 |
| #6 | 5'1" | 0.78 |
| D = 200' | 4'9" | 1.14 |
| T.D. =5'4" | 4'6" | 1.26 |
| I.T. = 1.9' | 4'3" | 1.37 |
| W.I. = 0 | 4'0" | 1.36 |
| | | 1.36 |
| | 3'9" | 1.35 |

TABLE A.2 CONTINUED

| SECTION | DEPTH | VELOCITY (fps) |
|---|---|---|
| | | 1.48 |
| | 3'6" | 1.32 |
| | | 1.35 |
| | 3'3" | 1.49 |
| | | 1.47 |
| | 3'0" | 1.48 |
| | 2'9" | 1.41 |
| | 2'6" | 1.38 |
| | 2'3" | 1.31 |
| | 2'0" | 1.21 |
| #7 | 5'1" | 1.01 |
| D = 250' | 4'9" | 1.19 |
| T.D. = 5'4" | 4'6" | 1.26 |
| I.T. = 1.9' | 4'3" | 1.35 |
| W.I. = 0 | 4'0" | 1.40 |
| | 3'9" | 1.45 |
| | 3'6" | 1.42 |
| | 3'3" | 1.50 |
| | 3'0" | 1.45 |
| | 2'9" | 1.49 |
| | 2'6" | 1.38 |
| | 2'3" | 1.32 |
| | 2'0" | 1.24 |

| SECTION | DEPTH | VELOCITY (fps) |
|---|---|---|
| | 1'11" | 0.94 |
| #8 | 5'10" | 0.88 |
| D = 300' | 5'6" | 1.03 |
| T.D. = 6'1" | 5'3" | 1.06 |
| I.T. = 1.6' | 4'9" | 1.21 |
| W.I. = 0 | 4'6" | 1.29 |
| | 4'3" | 1.31 |
| | 4'0" | 1.35 |
| | 3'9" | 1.36 |
| | 3'6" | 1.34 |
| | 3'3" | 1.44 |
| | 3'0" | 1.40 |
| | 2'9" | 1.40 |
| | 2'6" | 1.43 |
| | 2'3" | 1.37 |
| | 2'0" | 1.29 |
| | 1'8" | 0.92 |
| #9 | 4'7" | 0.63 |
| D = 350' | 4'3" | 1.13 |
| T.D. = 4'10" | 4'0" | 1.30 |
| I.T. = 1.95' | 3'9" | 1.43 |
| W.I. = 0 | 3'6" | 1.48 |
| | 3'3" | 1.54 |

TABLE A.2 CONTINUED

| SECTION | DEPTH | VELOCITY (fps) |
|---|---|---|
| | 3'0" | 1.56 |
| | 2'9" | 1.54 |
| | 2'6" | 1.50 |
| | 2'3" | 1.45 |
| | 2'1" | 0.99 |
| #10 | 5'6" | 0.79 |
| D = 400' | 5'3" | 0.81 |
| T.D. = 5'9" | 5'0" | 0.99 |
| I.T. = 1.4' | 4'9" | 1.07 |
| W.I. = 0 | 4'6" | 1.08 |
| | 4'3" | 1.12 |
| | 4'0" | 1.17 |
| | 3'9" | 1.19 |
| | 3'6" | 1.28 |
| | 3'3" | 1.32 |
| | 3'0" | 1.35 |
| | 2'9" | 1.37 |
| | 2'6" | 1.36 |
| | 2'3" | 1.40 |
| | 2'0" | 1.37 |
| | 1'9" | 1.30 |
| | 1'6" | 0.95 |

| SECTION | DEPTH | VELOCITY (fps) |
|---|---|---|
| #11 | 3'8" | 1.26 |
| D = 450' | 3'6" | 1.30 |
| T.D. = 3'11" | 3'3" | 1.80 |
| I.T. = 1.3' | 3'0" | 1.92 |
| W.I. = 0 | 2'9" | 2.08 |
| | 2'6" | 2.22 |
| | 2'3" | 2.33 |
| | 2'0" | 2.32 |
| | 1'9" | 2.25 |
| | 1'5" | 1.69 |
| #12 | 4'3" | 1.35 |
| D = 500' | 4'0" | 1.72 |
| T.D. = 4'6" | 3'9" | 2.00 |
| I.T. = 1.3' | 3'6" | 2.27 |
| W.I. = +0.5" | 3'3" | 2.45 |
| | 3'0" | 2.52 |
| | 2'9" | 2.72 |
| | 2'6" | 2.89 |
| | 2'3" | 2.97 |
| | 2'0" | 3.04 |
| | 1'9" | 2.80 |
| | 1'5" | 1.96 |

TABLE A.2 CONTINUED

| SECTION | DEPTH | VELOCITY (fps) |
|---|---|---|
| #13 | 5'0" | 0.61 |
| D = 550' | 4'9" | 1.02 |
| T.D. = 5'3" | 4'6" | 1.09 |
| I.T. = 1.5' | 4'3" | 1.36 |
| W.I. = +1.0" | 4'0" | 1.59 |
| | 3'9" | 1.64 |
| | 3'6" | 1.77 |
| | 3'3" | 1.89 |
| | 3'0" | 2.05 |
| | 2'9" | 2.23 |
| | 2'6" | 2.36 |
| | 2'3" | 2.27 |
| | 2'0" | 2.26 |
| | 1'9" | 2.05 |
| | 1'7" | 1.30 |
| #14 | 3'6" | 0.79 |

| SECTION | DEPTH | VELOCITY (fps) |
|---|---|---|
| D = 600' | 3'3" | 0.92 |
| T.D. = 3'9" | 3'0" | 1.14 |
| I.T. = 1.7' | 2'9" | 1.33 |
| W.I. = +0.5" | 2'6" | 1.43 |
| | 2'3" | 1.54 |
| | 2'0" | 1.34 |
| | 1'9" | 0.98 |
| #15 | 3'4" | 0.47 |
| D = 628' | 3'0" | 0.90 |
| T.D. = 3'7" | 2'9" | 1.04 |
| I.T. = 17' | 2'6" | 1.06 |
| W.I. = -1.0" | 2'3" | 1.05 |
| | 2'0" | 0.98 |
| | 1'9" | 0.71 |
| #16 D = 650' | FROZEN TO BOTTOM | |

D - DISTANCE FROM WEST BANK

TD - TOTAL DEPTH OF WATER

IT - ICE THICKNESS

WI - WATER LEVEL WITH RESPECT TO THE TOP OF THE ICE

# APPENDIX B

# DATA PROCESSING

## LINEAR REGRESSION

The values of velocity, x, and the logarithm of the depth, y, were fitted with a straight line by the method of least squares. The most probable position of such a line

$$x = a + by \quad \text{- - - - - - - - - - - (B-1)}$$

is such that the sum of the squares of the deviation of all points from the line is a minimum. For n observations this occurs when:

$$a = \frac{\Sigma y^2 \, \Sigma x - \Sigma y \Sigma xy}{n\Sigma y^2 - (\Sigma y)^2} \quad \text{- - - - (B-2)}$$

$$b = \frac{n\Sigma xy - \Sigma x \Sigma y}{n\Sigma y^2 - (\Sigma y)^2} \quad \text{- - - - - (B-3)}$$

As a test on the exactness of the fit, a correlation coefficient was computed,

$$C = \frac{n\Sigma xy - \Sigma x \Sigma y}{\sqrt{\left[n\Sigma x^2 - (\Sigma x)^2\right]\left[n\Sigma y^2 - (\Sigma y)^2\right]}} \quad \text{- - - - (B-4)}$$

## MANNING'S n FOR TOTAL CROSS-SECTION

Values of n were obtained at several sections across the cross-section. From these it was then necessary to obtain a n for the entire cross-section. The channel cross-section was divided into m sections with a measurement for each section. The sum of the discharges of each section must equal the total discharge.

$$Q = \sum_{i=1}^{m} dQ_i \quad \text{- - - - - - - - - - - (B-5)}$$

The sections are wide compared to the depth and the bed slope is constant, giving:

$$\frac{1.486}{n}\left(\frac{d}{2}\right)^{2/3} S^{1/2}\, db = \sum_{i=1}^{m} \frac{1.486}{n_i}\left(\frac{di}{2}\right)^{2/3} S^{1/2}\, d_i b_i \quad \text{- - (B-6)}$$

$$n = \frac{bd^{5/3}}{\sum_{i=1}^{m} \frac{b_i d_i^{5/3}}{n_i}} \quad \text{- - - - - - - - - - - - - - - - - (B-7)}$$

where:

$Q$ - total discharge

$dQ_i$ - discharge for each section

$n$ - Manning's n for the entire cross-section

$n_i$ - Manning's n for each section

$b$ - sum of the widths of all sections

$b_i$ - width of each section

$d$ - total cross-sectional area divided by b

$d_i$ - depth of each section.

TABLE B.1

AREA AND DISCHARGE CALCULATIONS

| Section | $b_i$ ft. | $d_i$ ft. | $b_i d_i$ $ft^2$ | $V_{Mean}$ ft/sec | $dQ_i = b_i d_i \cdot V_{Mean}$ cfs |
|---|---|---|---|---|---|
| 3 | 6.0 | 0.0 | 0.0 | 0.0 | 0.0 |
| 4 | 12.5 | 3.00 | 37.5 | 1.22 | 45.8 |
| 5 | 19.0 | 3.20 | 60.8 | 1.54 | 93.6 |
| 6 | 37.5 | 3.40 | 127.5 | 1.32 | 168.3 |
| 7 | 50.0 | 3.50 | 175.0 | 1.32 | 231.0 |
| 8 | 50.0 | 4.45 | 222.5 | 1.20 | 267.0 |
| 9 | 50.0 | 2.85 | 142.5 | 1.32 | 188.1 |
| 10 | 50.0 | 4.35 | 217.5 | 1.17 | 254.5 |
| 11 | 50.0 | 2.55 | 127.5 | 1.94 | 247.4 |
| 12 | 50.0 | 3.15 | 157.5 | 2.34 | 368.6 |
| 13 | 50.0 | 3.75 | 187.5 | 1.71 | 320.6 |
| 14 | 39.0 | 2.10 | 81.9 | 1.13 | 92.5 |
| 15 | 25.0 | 1.95 | 48.8 | 0.85 | 41.5 |
| 16 | 11.0 | 0.0 | 0.0 | 0.0 | 0.0 |

AVERAGE DEPTH = $\Sigma b_i d_i / \Sigma b_i$ = 3.17 FT.

TABLE B.2

REGRESSION ANALYSIS

| SECTION | BED BOUNDARY | | | ICE BOUNDARY | | |
|---|---|---|---|---|---|---|
| | X = A + BY | | CORRELATION COEFFICIENT | X = A + BY | | CORRELATION COEFFICIENT |
| | A | B | | A | B | |
| 4 | 1.2434 | 0.6549 | 0.975 | 1.4329 | 0.2814 | 0.999 |
| 5 | 1.5536 | 0.7301 | 0.991 | 1.8159 | 0.4915 | 0.989 |
| 6 | 1.2533 | 0.6669 | 0.950 | 1.4458 | 0.2337 | 0.983 |
| 7 | 1.3127 | 0.4876 | 0.984 | 1.4621 | 0.4095 | 0.956 |
| 8 | 1.1609 | 0.5115 | 0.985 | 1.3912 | 0.3963 | 0.965 |
| 9 | 1.3413 | 1.0894 | 0.989 | 1.6238 | 0.5121 | 0.931 |
| 10 | 1.0595 | 0.5838 | 0.979 | 1.4722 | 0.4647 | 0.984 |
| 11 | 1.9841 | 1.3575 | 0.982 | 2.4197 | 0.6506 | 0.980 |
| 12 | 2.2986 | 1.7512 | 0.993 | 3.2528 | 1.1974 | 1.000 |
| 13 | 1.4555 | 1.6342 | 0.978 | 2.4520 | 0.9587 | 0.955 |
| 14 | 1.3176 | 1.0010 | 0.977 | 1.6748 | 0.6503 | 0.997 |
| 15 | 1.0232 | 0.8175 | 0.950 | 1.1214 | 0.3668 | 0.984 |

TABLE B.3

COMPOSITE n

| SECTION | n FOR BED BOUNDARY | n FOR ICE BOUNDARY | COMPOSITE n | | | |
|---|---|---|---|---|---|---|
| | | | WEIGHTED AVERAGE | PAVLOVSKIY | BELOKAN & SABANEER | LARSEN |
| 4 | 0.0290 | 0.0098 | 0.0194 | 0.0217 | 0.0206 | 0.0184 |
| 5 | 0.0255 | 0.0140 | 0.0197 | 0.0206 | 0.0202 | 0.0201 |
| 6 | 0.0292 | 0.0081 | 0.0186 | 0.0215 | 0.0201 | 0.0158 |
| 7 | 0.0200 | 0.0146 | 0.0173 | 0.0176 | 0.0174 | 0.0173 |
| 8 | 0.0236 | 0.0149 | 0.0193 | 0.0198 | 0.0195 | 0.0193 |
| 9 | 0.0476 | 0.0167 | 0.0321 | 0.0358 | 0.0340 | 0.0302 |
| 10 | 0.0291 | 0.0167 | 0.0229 | 0.0238 | 0.0233 | 0.0220 |
| 11 | 0.0392 | 0.0137 | 0.0265 | 0.0295 | 0.0280 | 0.0266 |
| 12 | 0.0415 | 0.0203 | 0.0309 | 0.0328 | 0.0318 | 0.0315 |
| 13 | 0.0580 | 0.0219 | 0.0400 | 0.0440 | 0.0420 | 0.0419 |
| 14 | 0.0458 | 0.0219 | 0.0338 | 0.0360 | 0.0349 | 0.0349 |
| 15 | 0.0528 | 0.0174 | 0.0351 | 0.0395 | 0.0373 | 0.0307 |

TABLE B.4

MANNING'S n FOR ENTIRE CROSS-SECTION

| SECTION | $b_i d_i^{5/3}$ | WEIGHTED AVE. $\frac{b_i d_i^{5/3}}{n_i}$ | PAVLOVSKIY $\frac{b_i d_i^{5/3}}{n_i}$ | BELOKAN & SAB. $\frac{b_i d_i^{5/3}}{n_i}$ | LARSEN $\frac{b_i d_i^{5/3}}{n_i}$ |
|---|---|---|---|---|---|
| 4 | 78.0 | 4,020.6 | 3,594.5 | 3,786.4 | 4,239.1 |
| 5 | 132.0 | 6,700.5 | 6,407.8 | 6,534.7 | 6,567.2 |
| 6 | 288.3 | 15,500.0 | 13,409.3 | 14,343.3 | 18,246.8 |
| 7 | 403.4 | 23,317.9 | 22,920.5 | 23,183.9 | 23,317.9 |
| 8 | 602.0 | 31,191.7 | 30,404.0 | 30,871.8 | 31,191.7 |
| 9 | 286.4 | 8,922.1 | 8,000.0 | 8,423.5 | 9,483.4 |
| 10 | 579.6 | 25,310.0 | 24,352.9 | 24,875.5 | 26,345.5 |
| 11 | 238.0 | 8,981.1 | 8,067.8 | 8,500.0 | 8,947.4 |
| 12 | 338.4 | 10,951.5 | 10,317.1 | 10,641.5 | 10,742.9 |
| 13 | 452.6 | 11,315.0 | 10,286.4 | 10,776.2 | 10,801.9 |
| 14 | 134.3 | 3,973.4 | 3,730.6 | 3,848.1 | 3,848.1 |
| 15 | 76.1 | 2,168.1 | 1,926.6 | 2,040.2 | 2,478.8 |

WEIGHTED AVERAGE - n = 0.0225

PAVLOVSKIY - n = 0.0238

BELOKAN & SABANEER - n = 0.0231

LARSEN - n = 0.0219

# APPENDIX C

## COMPUTER PROGRAM

```
C                                WAV 21
C USES SUBROUTINES
C  INCLUDES THE CONDITION OF ICE COVER
      REAL MN
      COMMON XO(300,2),YO(300,2),T(251,2),X(251,2),V(251,2),Y(251,2),
     1HDG(20,4),VECT(1004),B,SO,XR,MN,TSCL,XSCL,SS,SI,NMX(2)
    1 WRITE(6,1000)
 1000 FORMAT('1',20X,'WAV21')
      TSCL=1./3600.
      XSCL=1./5280.
      READ(5,1001,END=999)B,XR,SO,MN,SS
 1001 FORMAT(5F15.6)
      SI=SS+SQRT(1.+SS*SS)
      WRITE(6,1002)B,XR,SO,MN,SS,SI
 1002 FORMAT('0B=',F10.3,5X,'XR=',F10.2,5X,'SO=',F10.6,5X,'MN=',F10.3,5X
     1,'SS=',F10.2,' SI=',F10.3)
C   READ IN TABULATED DATA
C   K=1 FOR TIME IN HRS (XO) VS DISCHARGE (YO) AT LEFT END
C EACH TABLE PRECEEDED BY HDG CARD & TERMINATED WITH XO=-9999.9
      K=1
    7 NMX(K)=0
      READ(5,1003)(HDG(J,K),J=1,20)
 1003 FORMAT(20A4)
      DO 10 I=1,300
      READ(5,1004)XO(I,K),YO(I,K)
 1004 FORMAT(2F10.3)
      IF(XO(I,K).EQ.-9999.9)GO TO 12
      NMX(K)=NMX(K)+1
   10 CONTINUE
   12 NX=(NMX(K)+11)/12
      WRITE(6,1015)K
 1015 FORMAT('0TABLE',I5)
      WRITE(6,1003)(HDG(J,K),J=1,20)
      I2=0
      DO 20 I=1,NX
      I1=I2+1
      I2=I1+11
      IF(I2.GT.NMX(K))I2=NMX(K)
      WRITE(6,1005)(XO(J,K),J=I1,I2)
 1005 FORMAT('0XO:',12F10.2)
      WRITE(6,1006)(YO(J,K),J=I1,I2)
 1006 FORMAT(' YO:',12F10.2)
   20 CONTINUE
      IF(K.EQ.2)GO TO 23
C TRANSFORM TIME IN HOURS TO TIME IN SECONDS
      K=NMX(1)
      DO 22 I=1,K
      XO(I,1)=XO(I,1)*3600.
   22 CONTINUE
C
C  READ IN STAGE-DISCHARGE CURVE AT DOWNSTREAM (RIGHT HAND) END
C  K=2 FOR DEPTH IN FEET (XO) AND FLOW IN CFS (YO)
C  CARDS RRECEEDED BY HDG CARD & TERMINATED WITH XO=-9999.9
      K=2
      GO TO 7
C  READ IN NO. OF INITIAL POINTS ON REACH & CALCULATE INITIAL CONDITION
   23 READ(5,1007)N,TMAX
 1007 FORMAT(I10,F10.2)
      WRITE(6,1013)N,TMAX
 1013 FORMAT('0N=',I5,5X,'TMAX=',F20.3,'  HOURS')
C  STORE B,XR,MN,SO,N,SS, & TMAX IN FIRST TAPE RECORD SPACE
      VECT(1)=B
      VECT(2)=XR
      VECT(3)=SO
```

```
      VECT(4)=MN
      VECT(5)=SS
      VECT(6)=10*N
      VECT(7)=TMAX
      WRITE(3) VECT
      XR=5280.*XR
      TMAX=TMAX*3600.
      IF(N.GT.250)N=250
      DX=XR/FLOAT(N-1)
C   INITIAL CONDITION  IS THE NORMAL FLOW & DEPTH CORRESPONDING TO THE
C         INITIAL UPSTREAM DISCHARGE
      QNORM=Y0(1,1)
      CALL DNORM(QNORM,MN,B,S0,SS,YNORM)
      CALL DCRIT(QNORM,B,SS,YCRIT)
      WRITE(6,1008)YNORM,YCRIT,QNORM
 1008 FORMAT('ONORMAL DEPTH=',F10.2,10X,'CRITICAL DEPTH=',F10.2,5X,'AT Q
     1=',F10.2)
C
C    SET UP INITIAL CONDITIONS
      AREA=YNORM*(B+YNORM*SS)
      V1=QNORM/(AREA)
      Y1=YNORM
      DO 30 I=1,N
      T(I,1)=0.0
      X(I,1)=DX*FLOAT(I-1)
      V(I,1)=V1
      Y(I,1)=Y1
   30 CONTINUE
      T(N+1,1)=-1.0
      CALL VECTR(N)
      WRITE(3) VECT
      IPNTR=1
      WRITE (6,1009)
 1009 FORMAT('0 INITIAL CONDITIONS')
      CALL SCRIB
      WRITE(6,1014)
 1014 FORMAT('   CALCULATED RESULTS')
      CALL SORT (IPNTR,YMAX,VMAX,VMIN)
C
   33 CALL REACH(1,IT)
      CALL SHIFT
C  VECTR(N) TRANSFERS T, X, V, & Y TO VECT & CHANGES T FROM HOURS TO
C    SECONDS  AND X FROM FEET TO MILES.
      CALL VECTR(N)
      WRITE(3) VECT
      IPNTR=IPNTR+1
      CALL SORT (IPNTR,YMAX,VMAX,VMIN)
      TM=T(1,1)
      XM=X(1,1)
      VM=V(1,1)
      YM=Y(1,1)
      CALL BDY1 (TM,XM,VM,YM,TN,XN,VN,YN)
      T(1,2)=TN
      X(1,2)=XN
      V(1,2)=VN
      Y(1,2)=YN
      CALL REACH(2,IT)
      TL=T(IT,1)
      XL=X(IT,1)
      VL=V(IT,1)
      YL=Y(IT,1)
      CALL BDY2 (TL,XL,VL,YL,TN,XN,VN,YN)
      IT=IT+1
      T(IT,2)=TN
      X(IT,2)=XN
      V(IT,2)=VN
```

```
      Y(IT,2)=YN
      T(IT+1,2)=-1.0
      CALL SHIFT
      CALL VECTR(N)
      WRITE(3) VECT
      IPNTR=IPNTR+1
      CALL SORT (IPNTR,YMAX,VMAX,VMIN)
C  FIND SMALLEST T CALCULATED IN LAST PASS
      TST=.99E 10
      DO 40 I=1,251
      IF(T(I,1).LT.0.)GO TO 41
      IF(T(I,1).LT.TST)TST=T(I,1)
   40 CONTINUE
C                 *
   41 IF(TST.LT.TMAX)GO TO 33
C                 *
      TX=TMAX*TSCL
      WRITE(6,1010)TST,TX
 1010 FORMAT('0 TST=',F10.2,5X,'TMAX=',F10.2,' *END OF XT PLANE CALCLN')
      WRITE(6,1020)
 1020 FORMAT('0 MAXIMUM AND MINIMUM VALUES FOR STEP1',/)
      WRITE(6,1021) YMAX, VMAX, VMIN
 1021 FORMAT('0',10X,'YMAX:',F8.2,10X,'VMAX:',F8.2,10X,'VMIN:',F8.2/)
C  FILL LAST RECORD WITH -1.0 VALUES
      DO 51 I=1,1004
      VECT(I)=-1.0
   51 CONTINUE
C     OVERWRITE VECT(1000) TO VECT(1002) WITH YMAX, VMAX, VMIN
      VECT(1000)=YMAX
      VECT(1001)=VMAX
      VECT(1002)=VMIN
      IPNTR=IPNTR+1
      WRITE(3) VECT
  999 WRITE(6,1012)IPNTR
 1012 FORMAT(' STEP1 COMPLETE',I20,'  RECORDS ON TAPE')
      CALL EXIT
      STOP
      END
      SUBROUTINE BDY1(TM,XM,VM,YM,TN,XN,VN,YN)
C  FOR TABULATED FLOW AT LEFT HAND END (N=1)  WITH ICE COVER
C  TRAPEZOIDAL CHANNEL WITH CONSTANT SLOPE
C  REQUIRES SUBROUTINE TABL4 WHICH RETURNS TWO VALUES OF Q ON EITHER
C  SIDE OF ESTIMATED TN.
C  THIS SUBROUTINE CALLED BDYILQ IN NOTES
      REAL MN
      COMMON X0(300,2),Y0(300,2),T(251,2),X(251,2),V(251,2),Y(251,2),
     1HDG(20,4),VECT(1004),B,S0,XR,MN,TSCL,XSCL,SS,SI,NMX(2)
C
C INITIALIZE
      B0=B
      XN=0.
      YN=YM
      VN=VM
      AM=YM*(B0+YM*SS)
      COM=SQRT(32.17*AM/(B0+2.*YM*SS))
      TN=TM-XM/(VM-COM)
      SFM=VM*VM*MN*MN*(2.*(B0+YM*SI)/(YM*(B0+YM*SS)))**1.333/2.22
      CALL TABL4(1,TN,TM2,QM2,TM1,QM1,TP1,QP1,TP2,QP2)
C  CURVES SMOOTHED BY TAKING AVERAGED POSITIONS
      QM2=(QM1+QM2)*0.5
      TM2=(TM1+TM2)*0.5
      QM1=(QM1+QP1)*0.5
      TM1=(TM1+TP1)*0.5
      QP1=(QP1+QP2)*0.5
      TP1=(TP1+TP2)*0.5
      QP2=QP2+QP2-QP1
```

```
      TP2=TP2+TP2-TP1
      ALFA=QM2/((TM2-TM1)*(TM2-TP1)*(TM2-TP2))
      BETA=QM1/((TM1-TM2)*(TM1-TP1)*(TM1-TP2))
      GAMA=QP1/((TP1-TM2)*(TP1-TM1)*(TP1-TP2))
      DELT=QP2/((TP2-TM2)*(TP2-TM1)*(TP2-TP1))
      A0=-ALFA*TM1*TP1*TP2-BETA*TM2*TP1*TP2-GAMA*TM2*TM1*TP2-DELT*TM2*
     1TM1*TP1
      A1=(GAMA+DELT)*TM2*TM1+(BETA+DELT)*TM2*TP1+(BETA+GAMA)*TM2*TP2
     1+(ALFA+DELT)*TM1*TP1+(ALFA+GAMA)*TM1*TP2+(ALFA+BETA)*TP1*TP2
      A2=(-BETA-GAMA-DELT)*TM2+(-ALFA-GAMA-DELT)*TM1+(-ALFA-BETA-DELT)*
     1TP1+(-ALFA-BETA-GAMA)*TP2
      A3=ALFA+BETA+GAMA+DELT
C  NOTE THE EQUATION  QN=A0+A1*TN+A2*TN*TN+A3*TN*TN*TN USES THE SAME
C   COEFFICIENTS FOR ALL ITERATIONS
      ITRN=0
      TTST=1.
      VTST=1.E-04
      YTST=1.E-04
C
   10 QN=((A3*TN+A2)*TN+A1)*TN+A0
      IF(QN.LT.0.)WRITE(6,1002)TN,QN
 1002 FORMAT(' BDY1,   TN=',E15.6,'  QN=',E15.6)
      AN=YN*(B0+YN*SS)
      VN=QN/AN
      PN=2.*(B0+YN*SI)
      BN=B0+2.*YN*SS
      SFN=1.13506*QN*QN*MN*MN*(B0+YN*SI)**1.333/((YN*(B0+YN*SS))**3.333)
      CON=SQRT(32.17*AN/BN)
      ITRN=ITRN+1
C
      F10=0.5*(COM+CON)*(VN-VM)-32.17*(YN-YM)+8.0425*(COM+CON)*(SFM-2.*
     1S0+SFN)*(TN-TM)
      F20=0.5*(TN-TM)*(VM-COM+VN-CON)+XM
      DF1DTN=0.5*(COM+CON)*(16.085*(SFM-2.*S0+SFN)+(1./AN+32.17*(TN-TM)*
     1SFN/QN)*(A1+2.*A2*TN+3.*A3*TN*TN))
      DF1DYN=-32.17+4.02125*(1.-2.*SS*AN/(BN*BN))*(2.*(VN-VM)+32.17*(TN-
     1TM)*(SFM-2.*S0+SFN))/CON+9.651*(TN-TM)*(COM+CON)*QN*QN*MN*MN*PN**0
     1.333*(SI-1.25*PN*BN/AN)/(AN**3.333)-QN*BN/(2.*AN*AN)*(COM+CON)
      DF2DTN=0.5*(VM-COM+VN-CON+(TN-TM)*(A1+2.*A2*TN+3.*A3*TN*TN)/AN)
      DF2DYN=0.5*(TM-TN)*(VN*BN/AN+16.085*(1.-2.*SS*AN/(BN*BN))/CON)
      DEN=DF1DTN*DF2DYN-DF1DYN*DF2DTN
      DT=(F20*DF1DYN-F10*DF2DYN)/DEN
      DY=(F10*DF2DTN-F20*DF1DTN)/DEN
      TN=TN+0.5*DT
      YN=YN+0.5*DY
      IF(ITRN.GT.40)GO TO 17
      IF((DT.GT.TTST).OR.(DY.GT.YTST))GO TO 10
      GO TO 20
   17 WRITE(6,1001)ITRN
 1001 FORMAT('0',I10,' ITERATIONS IN BDY1, STOP')
      STOP
   20 QN=((A3*TN+A2)*TN+A1)*TN+A0
      VN=QN/(YN*B0+YN*YN*SS)
      TTN=TN/3600.
      WRITE(6,1003)TTN,QN
 1003 FORMAT(' UPSTREAM END, T=',E15.6,' Q=',E15.6,' C.F.S.')
      RETURN
      END
      SUBROUTINE REACH (II,IT)
C  CALCULATES INTERIOR POINTS ON X-T DIAGRAM
C  II IS INDEX NUMBER OF FIRST POINT CALCULATED
C  IT IS INDEX NUMBER OF LAST POINT CALCULATED
      REAL MN
      COMMON XO(300,2),YO(300,2),T(251,2),X(251,2),V(251,2),Y(251,2),
     1HDG(20,4),VECT(1004),B,S0,XR,MN,TSCL,XSCL,SS,SI,NMX(2)
      K=II-1
```

```
      G=32.17
      DO 100 I=1,250
      MIT=0
      IF(T(I+1,1).LT.-0.1)GO TO 110
      TL=T(I,1)
      XL=X(I,1)
      VL=V(I,1)
      YL=Y(I,1)
      TM=T(I+1,1)
      XM=X(I+1,1)
      VM=V(I+1,1)
      YM=Y(I+1,1)
      AL=YL*(B+YL*SS)
      PL=B+2.*YL*SQRT(1.+SS*SS)+B+2.*YL*SS
      SFL= VL*VL*MN*MN/(2.22*(AL/PL)**1.3333)
      AM=YM*(B+YM*SS)
      PM=B+2.*YM*SQRT(1.+SS*SS)+B+2.*YM*SS
      SFM= VM*VM*MN*MN/(2.22*(AM/PM)**1.3333)
C
      XN=0.5*(XL+XM)
      VN=0.5*(VL+VM)
      YN=0.5*(YL+YM)
      CLO=SQRT(32.17*AL/(B+2.*YL*SS))
      CMO=SQRT(32.17*AM/(B+2.*YM*SS))
      TN=TL+(XN-XL)/(VL+CLO)
C
   10 AN=YN*(B+YN*SS)
      PN=2.*B+2.*YN*SQRT(1.+SS*SS)+2.*YN*SS
      BN=B+2.*YN*SS
      SFN=VN*VN*MN*MN/2.22*(PN/AN)**1.3333
      CNO=SQRT(G*AN/(B+2.*YN*SS))
      COP=CLO+CNO
      COM=CMO+CNO
       ISW=1
       F1T=0.5*(VL+VN+COP)
       F1X=-1.0
       F1V=0.5*(TN-TL)
       F1Y=G/(4.*CNO)*(TN-TL)*(1.-2.*SS*AN/(BN*BN))
       F2T=0.5*(VM+VN-COM)
       F2X=-1.0
       F2V=0.5*(TN-TM)
       F2Y=-G/(4.*CNO)*(TN-TM)*(1.-2.*SS*AN/(BN*BN))
       F3T=G/4.*COP*(SFL+SFN-2.*SO)
       F3V=0.5*COP+G*COP/4.44*(TN-TL)*VN*MN*MN*(PN/AN)**1.3333
       F3Y=(0.5*(VN-VL)+G/4.*(TN-TL)*(SFL-2.*SO+SFN))*(G/(2.*CNO))*(1.-2.
     1*SS*AN/(BN*BN))+G+G/3.33*(TN-TL)*COP*VN*VN*MN*MN*(PN/AN)**0.3333*(
     2SI/AN-PN*BN/(2.*AN*AN))
       F4T=G/4.*COM*(SFM-2.*SO+SFN)
       F4V=0.5*COM+G/4.44*COM*(TN-TM)*VN*MN*MN*(PN/AN)**1.3333
       F4Y=(0.5*(VN-VM)+G/4.*(TN-TM)*(SFM-2.*SO+SFN))*(G/(2.*CNO))*(1.-2.
     1*SS*AN/(BN*BN))-G+G/3.33*(TN-TM)*COM*VN*VN*MN*MN*(PN/AN)**0.3333*(
     2SI/AN-PN*BN/(2.*AN*AN))
       F10=-1.*(0.5*(TN-TL)*(VL+VN+COP)-(XN-XL))
       F20=-1.*(0.5*(TN-TM)*(VM+VN-COM)-(XN-XM))
       F30=-1.*(0.5*COP*(VN-VL)+G*(YN-YL)+G*0.5*COP*((SFL+SFN)*0.5-SO)*(T
     1N-TL))
       F40=-1.*(0.5*COM*(VN-VM)-G*(YN-YM)+G*0.5*COM*((SFM+SFN)*0.5-SO)*(T
     1N-TM))
       F110=F20-F10
       F11T=F2T-F1T
       F11V=F2V-F1V
       F11Y=F2Y-F1Y
       DET=F11T*(F3V*F4Y-F3Y*F4V)+F11V*(F3Y*F4T-F3T*F4Y)+F11Y*(F3T*F4V-F3
     1V*F4T)
       DELT=F110*(F3V*F4Y-F3Y*F4V)+F11V*(F3Y*F40-F30*F4Y)+F11Y*(F30*F4V-F
     13V*F40)
```

```
      DELV=F11T*(F30*F4Y-F3Y*F40)+F110*(F3Y*F4T-F3T*F4Y)+F11Y*(F3T*F40-F
     130*F4T)
      DELY=F11T*(F3V*F40-F30*F4V)+F11V*(F30*F4T-F3T*F40)+F110*(F3T*F4V-F
     13V*F4T)
      DT=DELT/DET
      DV=DELV/DET
      DY=DELY/DET
      T1=TN+DT
      V1=VN+DV
      Y1=YN+DY
      X1=XL+((T1-TL)/2.)*(VL+CLO+V1+SQRT(G*Y1*(B+Y1*SS)/(B+2.*Y1*SS)))
      MIT=MIT+1
      IF (MIT .LT. 10) GO TO 20
      WRITE(6,1000) MIT,I
      WRITE(6,1001)TN,XN,YN,VN,T1,X1,Y1,V1
      WRITE(6,1001)F10,F20,F30,F40,DET,DELT,DELV,DELY
1000  FORMAT(2X,'I=',I5,10X,'MIT=',I5)
1001  FORMAT(1X,8E14.6)
   20 GO TO (30,40,50,60),ISW
   30 TST=ABS(T1-TN)-1.0
      GO TO 70
   40 TST=ABS(X1-XN)-10.0
      GO TO 70
   50 TST=ABS(V1-VN)-1.0E-4
      GO TO 70
   60 TST=ABS(Y1-YN)-1.0E-4
   70 IF(TST.GT.0.)GO TO 80
      ISW=ISW+1
      IF(ISW.LT.5) GO TO 20
   80 TN=T1
      XN=X1
      YN=Y1
      VN=V1
      IF(ISW.LT.5)GO TO 10
      K=K+1
      T(K,2)=TN
      X(K,2)=XN
      V(K,2)=VN
      Y(K,2)=YN
  100 CONTINUE
C
  110 IT=K
      T(IT+1,2)=-1.0
      RETURN
      END
      SUBROUTINE BDY2(TL,XL,VL,YL,TN,XN,VN,YN)
C  FOR TABULATED STAGE-DISCHARGE CURVE AT RIGHT HAND END OF CHANNEL
C  (DOWNSTREAM END). TRAPEZOIDAL CROSS-SECTION WITH CONSTANT SLOPE.
C  REQUIRES SUBROUTINE TABL4 WITH N=2.
      REAL MN
      COMMON XC(300,2),YO(300,2),T(251,2),X(251,2),V(251,2),Y(251,2),
     1HDG(20,4),VECT(1004),B,SO,XR,MN,TSCL,XSCL,SS,SI,NMX(2)
C
C     INITIALIZE
      BO=B
      XN=XR
      AL=YL*(BO+YL*SS)
      BL=BO+2.*YL*SS
      PL=2.*(BO+YL*SI)
      COL=SQRT(32.17*AL/BL)
      SFL=VL*VL*MN*MN*(PL/AL)**1.333/2.22
      TN=TL+(XN-XL)/(VL+COL)
      YN=YL
      CALL TABL4(2,YN,YM2,QM2,YM1,QM1,YP1,QP1,YP2,QP2)
      ALFA=QM2/((YM2-YM1)*(YM2-YP1)*(YM2-YP2))
      BETA=QM1/((YM1-YM2)*(YM1-YP1)*(YM1-YP2))
```

```
      GAMA=QP1/((YP1-YM2)*(YP1-YM1)*(YP1-YP2))
      DELT=QP2/((YP2-YM2)*(YP2-YM1)*(YP2-YP1))
      A0=-ALFA*YM1*YP1*YP2-BETA*YM2*YP1*YP2-GAMA*YM2*YM1*YP2-DELT*YM2*
     1YM1*YP1
      A1=(GAMA+DELT)*YM2*YM1+(BETA+DELT)*YM2*YP1+(BETA+GAMA)*YM2*YP2+
     1(ALFA+DELT)*YM1*YP1+(ALFA+GAMA)*YM1*YP2+(ALFA+BETA)*YP1*YP2
      A2=(-BETA-GAMA-DELT)*YM2+(-ALFA-GAMA-DELT)*YM1+(-ALFA-BETA-DELT)*
     1YP1+(-ALFA-BETA-GAMA)*YP2
      A3=ALFA+BETA+GAMA+DELT
C
C  NOTE THE EXPRESSION QN=A0+A1*YN+2.*YN**2+A3*YN**3 IS USED WITH THE
C   SAME COEFFICIENTS FOR ALL ITERATIONS.
      ITRN=0
      TTST=1.
      YTST=1.E-04
   10 QN=((A3*YN+A2)*YN+A1)*YN+A0
      AN=YN*(B0+YN*SS)
      BN=B0+2.*YN*SS
      PN=2.*(B0+YN*SI)
      SFN=1.13506*QN*QN*MN*MN*(B0+YN*SI)**1.333/((YN*(B0+YN*SS))**3.333)
      CON=SQRT(32.17*AN/BN)
      VN=QN/AN
      ITRN=ITRN+1
C
      DF1DTN=8.0425*(COL+CON)*(SFL-2.*S0+SFN)
      DF2DTN=0.5*(VL+COL+VN+CON)
C
      DF1DYN=0.5*(COL+CON)*(AN*(A1+2.*A2*YN+3.*A3*YN*YN)-QN*BN)/(AN*AN)+
     132.17+(0.5*(VN-VL)+8.0425*(TN-TL)*(SFL-2.*S0+SFN))*16.09*(1.-2.*SS
     2*AN/(BN*BN))/CON+9.660*(TN-TL)*(COL+CON)*QN*MN*MN*PN**0.333*(SI+0.
     375*PN*(3.*A3*YN*YN+2.*A2*YN+A1)-1.25*PN*QN*BN/AN)/(AN**3.333)
C
      DF2DYN=0.5*(TN-TL)*((A1+2.*A2*YN+3.*A3*YN*YN)/AN-QN*BN/(AN*AN)+
     116.085*(1.-2.*SS*AN/(BN*BN))/CON)
C
      F10=0.5*(COL+CON)*(VN-VL)+32.17*(YN-YL)+8.0425*(COL+CON)*(SFL-2.*
     1S0+SFN)*(TN-TL)
      F20=0.5*(TN-TL)*(VL+COL+VN+CON)-XR+XL
C
      DEN=DF1DTN*DF2DYN-DF1DYN*DF2DTN
      DT=(F20*DF1DYN-F10*DF2DYN)/DEN
      DY=(F10*DF2DTN-F20*DF1DTN)/DEN
C
      TN=TN+0.5*DT
      YN=YN+0.5*DY
      IF(ITRN.GT.24)GO TO 17
      IF((DT.GT.TTST).OR.(DY.GT.YTST))GO TO 10
      GO TO 20
   17 WRITE(6,1001)ITRN
 1001 FORMAT('0',I10,'  ITERATIONS IN BDY2,    *STOP*')
      STOP
   20 QN=((A3*YN+A2)*YN+A1)*YN+A0
      AN=YN*(B0+YN*SS)
      VN=QN/AN
      RETURN
      END
      SUBROUTINE TABL4(N,XP,XM2,YM2,XM1,YM1,XP1,YP1,XP2,YP2)
C  FINDS TWO PAIRS OF POINTS ON EITHER SIDE OF TN
C  TAKES DATA FROM TABLE N. NM(N) IS NUMBER OF TABLE ENTRIES IN TABLE N
C  RETURNS WITH TWO POINTS ON EITHER SIDE OF XP. EXCEPT NEAR END POINTS
C  WHERE THE FOUR END POINTS ARE RETURNED IF TN INSIDE RANGE OF DATA.
      REAL MN
      COMMON XO(300,2),YO(300,2),T(251,2),X(251,2),V(251,2),Y(251,2),
     1HDG(20,4),VECT(1004),B,S0,XR,MN,TSCL,XSCL,SS,SI,NMX(2)
      NM=NMX(N)
      IF((XP.LT.XO(2,N)).OR.(XP.GT.XO(NM-1,N)))GO TO 20
```

```
      M=NM-2
      DO 10 J=2,M
      I=J
      IF((XO(J,N).LE.XP).AND.(XO(J+1,N).GE.XP))GO TO 5
   10 CONTINUE
    5 XM2=XO(I-1,N)
      YM2=YO(I-1,N)
      XM1=XO(I,N)
      YM1=YO(I,N)
      XP1=XO(I+1,N)
      YP1=YO(I+1,N)
      XP2=XO(I+2,N)
      YP2=YO(I+2,N)
      GO TO 99
C
   20 IF((XP.LT.XO(1,N)).OR.(XP.GT.XO(NM,N)))GO TO 30
      IF(XP.LT.XO(2,N))GO TO 25
      I=NM-2
      GO TO 5
C
   25 I=2
      GO TO 5
C
   30 WRITE(6,1002)XP,N
 1002 FORMAT('0OUTSIDE RANGE IN TABL4, XP=',E15.6,'  N=',I5)
   99 RETURN
      END
      SUBROUTINE SORT (IPNTR,YMAX,VMAX,VMIN)
C     FINDS MAX DEPTH AND WRITES OUT T, X, V, & Y AT THIS POINT
C     FINDS MAX DEPTH AND VELOCITY AND MIN VELOCITY FOR TOTAL TIME
C     THESE VALUES CALCULATED ARE USED TO SET THE SCALES FOR PLOT
      REAL MN
      INTEGER AA,BB,CC
      COMMON XO(300,2),YO(300,2),T(251,2),X(251,2),V(251,2),Y(251,2),
     1HDG(20,4),VECT(1004),B,SO,XR,MN,TSCL,XSCL,SS,SI,NMX(2)
C     COUNT THE NO. OF VALUES CALCULATED
      N=0
      DO 10 I=1,251
      IF(VECT(4*I-3).LT.0.)GO TO 15
      N=N+1
   10 CONTINUE
   15 AA=4
      DO 20 K=2,N
      IF (VECT(4*K) .GT. VECT(AA)) GO TO 16
      GO TO 20
   16 AA=4*K
   20 CONTINUE
      BB=3
      DO 30 K=2,N
      IF (VECT(4*K-1) .GT. VECT(BB)) GO TO 26
      GO TO 30
   26 BB=4*K-1
   30 CONTINUE
      CC=3
      DO 40 K=2,N
      IF (VECT(4*K-1) .LT. VECT(CC)) GO TO 36
      GO TO 40
   36 CC=4*K-1
   40 CONTINUE
      WRITE(6,2000) IPNTR, VECT(AA-3), VECT(AA-2), VECT(AA-1), VECT(AA)
 2000 FORMAT('0',5X,' STEP:',I5,10X,' T:',F8.3,10X,' X:',F8.2,10X,' V:',
     1F8.2,10X,' YMAX:',F8.2)
      IF (IPNTR .LE. 1) GO TO 50
      IF (YMAX .LT. VECT(AA)) YMAX=VECT(AA)
      IF (VMAX .LT. VECT(BB)) VMAX=VECT(BB)
      IF (VMIN .GT. VECT(CC)) VMIN=VECT(CC)
```

```
      GO TO 60
   50 YMAX=VECT(AA)
      VMAX=VECT(BB)
      VMIN=VECT(CC)
   60 RETURN
      END
      SUBROUTINE SCRIB
C  WRITES OUT T,X,V,& Y FROM VECT
      REAL MN
      COMMON XC(300,2),YO(300,2),T(251,2),X(251,2),V(251,2),Y(251,2),
     1HDG(20,4),VECT(1004),B,SO,XR,MN,TSCL,XSCL,SS,SI,NMX(2)
C     COUNT NO. OF VALUES TO BE PRINTED OUT
      N=0
      DO 10 I=1,251
      IF(VECT(4*I-3).LT.0.)GO TO 15
      N=N+1
   10 CONTINUE
   15 NX=(N+11)/12
      I2=0
      DO 20 I=1,NX
      I1=I2+1
      I2=I1+11
      IF(I2.GT.N)I2=N
      WRITE(6,1000)(VECT(4*K-3),K=I1,I2)
 1000 FORMAT('0T:',12F10.3)
      WRITE(6,1001)(VECT(4*K-2),K=I1,I2)
 1001 FORMAT(' X:',12F10.2)
      WRITE(6,1002)(VECT(4*K-1),K=I1,I2)
 1002 FORMAT(' V:',12F10.2)
      WRITE(6,1003)(VECT(4*K),K=I1,I2)
 1003 FORMAT(' Y:',12F10.2)
   20 CONTINUE
      RETURN
      END
      SUBROUTINE SHIFT
C  SHIFTS THE INDEX VALUES ON CALCULATED POINTS
      REAL MN
      COMMON XC(300,2),YO(300,2),T(251,2),X(251,2),V(251,2),Y(251,2),
     1HDG(20,4),VECT(1004),B,SO,XR,MN,TSCL,XSCL,SS,SI,NMX(2)
      DO 10 I=1,251
      T(I,1)=T(I,2)
      X(I,1)=X(I,2)
      V(I,1)=V(I,2)
      Y(I,1)=Y(I,2)
      IF(T(I,1).LT.0.)GO TO 99
   10 CONTINUE
   99 RETURN
      END
      SUBROUTINE VECTR(N)
C  STORES CALCULATED POINTS
      REAL MN
      COMMON XC(300,2),YO(300,2),T(251,2),X(251,2),V(251,2),Y(251,2),
     1HDG(20,4),VECT(1004),B,SO,XR,MN,TSCL,XSCL,SS,SI,NMX(2)
      IPNTR=0
      M=N+1
      DO 10 I=1,M
      IPNTR=IPNTR+1
      VECT(IPNTR)=T(I,1)*TSCL
      IF (T(I,1) .LT. -0.1) GO TO 10
      IPNTR=IPNTR+1
      VECT(IPNTR)=X(I,1)*XSCL
      IPNTR=IPNTR+1
      VECT(IPNTR)=V(I,1)
      IPNTR=IPNTR+1
      VECT(IPNTR)=Y(I,1)
   10 CONTINUE
```

```
      RETURN
      END
      SUBROUTINE DNORM(Q,N,B,SO,SS,YNORM)
C CALCULATES NORMAL DEPTH IN TRAPEZOIDAL CHANNEL
      REAL N
C  INITIAL ESTIMATE OF YNORM IS 1.0 FT.
      ICT=1
      YNORM=1.0
      WO=Q*Q*N*N/(2.22*SO)
      SB=SQRT(1.+SS*SS)*2.0
    1 Y=YNORM
      A=Y*(B+Y*SS)
      P=B+Y*SB+B+2.*Y*SS
      R=A/P
      W=A*A*R**1.3333
      DW=W-WO
      DY=-3.*A*DW/(W*(10.*(B+2.*Y*SS)-4.*R*(SB+2.*SS)))
      YNORM =YNORM+DY
      TST=ABS(DY/YNORM)
      IF(TST.LE.1.0E-4)GO TO 99
      ICT=ICT+1
      IF (ICT .LT. 20) GO TO 1
      WRITE(6,1000) ICT,YNORM
 1000 FORMAT(2X,'ICT=',I5,10X,'YNORM=',E14.6)
      GO TO 1
   99 RETURN
      END
      SUBROUTINE DCRIT(Q,B,SS,YCRIT)
C CALCULATES CRITICAL DEPTH IN  TRAPEZOIDAL CHANNELS
C  INITIAL ESTIMATE OF YCRIT IS 1.0 FT.
      YCRIT=1.0
      WO=Q*Q/32.17
    1 Y=YCRIT
      A=Y*(B+Y*SS)
      S=B+2.*Y*SS
      W=A*A*A/S
      DW=W-WO
      DY=-DW*S*S/(A*A*(3.*S*S-2.*A*SS))
      YCRIT=YCRIT+DY
      TST=ABS(DY/YCRIT)
      IF(TST.LE.1.0E-6)GO TO 99
      GO TO 1
   99 RETURN
      END
```